High-energy flood events recorded in the Mesoproterozoic Meall Dearg Formation, NW Scotland; their recognition and implications for the study of pre-vegetation alluvium

William J. McMahon*, Neil S. Davies

University of Cambridge, Department of Earth Sciences, Downing Street, Cambridge CB2 3EQ, United Kingdom

*wjm39@cam.ac.uk

ABSTRACT

The Mesoproterozoic-Neoproterozoic Torridonian Sandstone of NW Scotland has renewed sedimentological significance following recent advances in the understanding of pre-vegetation alluvium, as it is one of the most extensive and easily-accessible successions of such strata worldwide. This paper presents the first modern sedimentological analysis of the unit's constituent Meall Dearg Formation (late Mesoproterozoic), recognizing a dominance of alluvial facies, with subordinate aeolian facies. Alluvial strata within the Meall Dearg Formation contain direct evidence for event deposition by high-energy floods, including: (1) widespread upper- and transitional-upper flow regime elements; (2) frequent stacking of successively-lower flow-regime elements; (3) common subcritical subaqueous dune fields with superimposed ripple marks; (4) occasional thin, desiccated mudstones; and (5) evidence that microbial mats colonized substrates during intervals of sedimentary stasis. Together these strands of primary sedimentary geological evidence indicate that the alluvial deposition of the Meall Dearg Formation was typified by supercritical flows during high-energy floods, punctuated by prolonged intervals of sedimentary stasis. The preservation potential of all of the features was boosted by highly aggradational sedimentary conditions. These primary observations have implications for the 'norm' in pre-vegetation alluvium and confirm that, despite increasing recognition of diversity within Precambrian fluvial systems, classical pre-vegetation motifs of high-energy alluvial flood deposits preserved as "sheet-braided" alluvium are still an archetypal

27   sedimentary signature in some instances. Using supportive evidence from the Meall Dearg

28   Formation, we recommend that the term "sheet-braided" be used in inverted commas in future

29   studies; this emphasises the polygenetic depositional nature of the 20:1 width:thickness fluvial

30   style, while maintaining the value of the term in the isolation of a key characteristic of pre-

31   vegetation sedimentary architecture.

34

35   **1. THE TORRIDONIAN SANDSTONE AND PRE-VEGETATION ALLUVIUM**

36   The 'Torridonian Sandstone' (or, simply 'the Torridonian') is the informal stratigraphic name

37   for a >10 km thick succession of Proterozoic siliciclastic strata, overlying the Archean Lewisian

38   gneiss complex, in the Highland region of northwest Scotland (Fig. 1). The Torridonian has been

39   a well-studied unit of British regional stratigraphy for almost 200 years (e.g., MacCulloch, 1819;

40   Sedgwick and Murchison, 1828; Peach et al., 1907). Its historical renown arises from both its

41   wide geographic outcrop extent (200 km north to south; even greater at subcrop ((Blundell et

42   al., 1985; Stein, 1988, 1992; Williams and Foden, 2011)) and status as the oldest

43   unmetamorphosed sedimentary rock in the British Isles. During the last fifty years, numerous

44   studies have concerned themselves with the sedimentary history of the succession (e.g., Selley,

45   1965; Williams, 1966, 2001; Gracie and Stewart, 1967; Stewart, 1969, 1982; Nicholson, 1993;

46   McManus and Bajabaa, 1998; Owen and Santos, 2014; Ielpi and Ghinassi, 2015; Ielpi et al., 2016;

47   Santos and Owen, 2016), its provenance and geochemistry (e.g., Stewart, 1991; Stewart and

48   Donnellan, 1992; Van de Kamp and Leake, 1997; Young, 1999; Williams and Foden, 2011), and

49   its palaeomagnetic (e.g., Stewart and Irving, 1974; Smith et al., 1983; Williams and Schmidt,

50   1997) and tectonostratigraphic (Kinnaird et al., 2007) characteristics. More recently, the

51   succession has seen a revival of palaeobiological interest: microfossils extracted from

52   Torridonian mudstones, first described by Teall (1907), have been deemed to the Earth's oldest

53 non-marine eukaryotes (Strother et al., 2011; Battison and Brasier, 2012; Brasier et al., 2016)

54 and indirect evidence for early microbial life on land has been described (Prave, 2002; Callow et

55 al., 2011; Strother and Wellman, 2016).

56 The Torridonian is also of global significance within a sedimentological context; containing

57 some of the most extensive and easily-accessible successions of pre-vegetation alluvial strata

58 worldwide. It is widely appreciated that river processes would have been markedly different

59 before land plant evolution, supported by observations in poorly-vegetated modern catchments

60 (e.g., Schumm, 1968; Fuller, 1985; Corenblit et al., 2015 ; Horton et al., 2017) and in the deep

61 time alluvial stratigraphic record (Cotter, 1978; Davies and Gibling, 2010; Gibling et al., 2014;

62 Davies et al., 2017a). A recent burst of geological investigations into pre-vegetation alluvium

63 has been driven by a demand for a better understanding of economically-significant

64 Precambrian and lower Palaeozoic hydrocarbon reservoirs and placer deposits, a search for

65 terrestrial analogues for extraterrestrial alluvium on planets such as Mars, and context for the

66 fossil record of the earliest life on Earth. A number of these studies have demonstrated the

67 existence of a much greater variability of pre-vegetation fluvial styles than has traditionally

68 been appreciated (e.g., Santos et al., 2014; Marconato et al., 2014; Ielpi and Rainbird, 2016a,

69 2016b; Santos and Owen, 2016) emphasising that further investigation of these anactualistic

70 sedimentary systems is needed to fully appreciate the diversity of Precambrian alluvium.

71 This paper contributes new data to the global pool of pre-vegetation studies, through an original

72 sedimentological analysis of the least-studied constituent unit of the Torridonian Sandstone: the

73 Mesoproterozoic Meall Dearg Formation (MDF). Considering the long history of geological

74 investigation into the region, and the number of studies that have focused on the more well-

75 known alluvial formations of the Torridonian (e.g., the Applecross [Selley, 1965; Nicholson,

76 1993; Owen, 1995; Stewart, 2002; Owen and Santos, 2014; Ielpi and Ghinassi, 2015; Santos and

77 Owen, 2016] and Bay of Stoer [Stewart, 1990; Stewart, 2002; Ielpi et al., 2016] formations), the

78 MDF has remained largely overlooked. This is the first paper to explicitly address the

79 sedimentary characteristics of the MDF, as only three studies have previously considered the

80   formation: Gracie and Stewart (1967) discussed sedimentary deposits at Enard Bay, Prave

81   (2002) discussed putative microbially-induced sedimentary structures, and Stewart (2002)

82   provided an overview of the MDF as part of a survey of the entire Torridonian. Other studies

83   have overlooked the MDF, potentially because of its limited exposure (cropping out at only four

84   locations; Rubha Réidh, Stoer, Balchladich Bay and Enard Bay) and dissection by the regionally-

85   significant Coigach Fault (Fig. 1). Existing interpretations of the MDF have suggested that it was

86   deposited by a sandy bedload-dominated fluvial system (Gracie and Stewart, 1967; Stewart,

87   2002). This paper revisits the formation in light of recent sedimentological advances, and

88   discusses: (1) the architectural characteristics of the constituent sand-bodies of the MDF; (2)

89   the spatial distribution of stratification types in accordance to established flow regime models;

90   (3) the variety of preserved bedding plane features within the MDF; and (4) recurring facies

91   that record prevailing sedimentary processes.   These novel observations permit the

92   interpretation of the MDF as recording distinct signatures of dominant high-energy alluvial

93   event (and subordinate aeolian) sedimentation, preserved due to exceptional aggradational

94   conditions.

95

96   **2. STRATIGRAPHIC AND GEOLOGICAL CONTEXT**

97   A detailed stratigraphy for the whole Torridonian is presented in Stewart (2002), and only a

98   brief overview of the stratigraphic context of the MDF is discussed here. The Torridonian

99   Sandstones comprise, from oldest to youngest, the Stoer, Sleat and Torridon groups (Fig. 1C); of

100   which the MDF is the youngest constituent formation of the >2000 m-thick Stoer Group. The

101   MDF succeeds the Bay of Stoer Formation and is unconformably overlain by the lacustrine

102   Diabaig Formation of the Torridon Group. The Bay of Stoer Formation consists of dominantly

103   fluvial, and subordinate interpreted aeolian (Park et al., 2002; Ielpi et al., 2016) sandstones.

104   Specifically, the MDF succeeds the shallow lacustrine Poll a'Mhuilt Member of the Bay of Stoer

105   Formation, apparently conformably. Lithostratigraphic correlation between the scattered

106   outcrops of the MDF is permitted by their common stratigraphic position above the Stac Fada

107   Member of the upper Bay of Stoer Formation, which comprises a regionally-extensive event bed

108   of meteorite-impact ejecta origin (Amor et al., 2008; Simms, 2015). However, the possibility

109   remains that the units at each locality are not necessarily time equivalents. The MDF has not

110   been directly dated, but its age is stratigraphically bracketed between 1177±5 Ma (Stenian

111   Period of the Mesoproterozoic) and 977±39 Ma (Tonian Period of the Neoproterozoic), based

112   on ^{40}Ar/^{39}Ar dating of the underlying Stac Fada Member and Rb-Sr whole-rock regressions of

113   the overlying Diabaig Formation (Turnbull et al., 1996; Parnell et al., 2011). This age indicates

114   that the MDF was deposited during the Grenvillian Orogeny, along the margins of the

115   supercontinent Rodinia (Rainbird et al., 2012). This deposition on the edge of the Laurentian

116   Shield meant that it largely avoided later Caledonian deformation (Williams and Foden, 2011).

117   The MDF is interpreted to have been deposited in a narrow rift basin with detritus sourced from

118   local fault scarps (Stewart, 1982, 1990; Rainbird et al., 2001). Palaeomagnetic (Torsyik and

119   Sturt, 1987) and geochemical (Stewart, 1990) data suggest deposition occurred in a semi-arid

120   climate at a palaeolatitude of 10-20°N. A glacial setting was proposed for the lowermost

121   Clachtoll Formation by Davison and Hambrey (1996), but evidence for this was disputed by

122   Stewart (1997) and Young (1999).

123

124   **3. SEDIMENTOLOGY OF THE MEALL DEARG FORMATION**

125

126   **Facies Associations**

127   Two facies associations (FA) are recognised in strata of the MDF (Fig. 2). The facies associations

128   are mutually exclusive, with FA1 cropping out at Rubha Réidh, Balchladich Bay and Stoer and

129   FA2 at Enard Bay.

130   **3.1. Facies Association 1 (Rubha Réidh, Balchladich Bay and Stoer)**

131   Strata of FA1 form the majority of the exposed MDF, and all of the facies at Rubha Réidh,

132   Balchladich Bay and Stoer. The contiguous Stoer-Balchladich Bay section is 200-300 m thick,

133 underlain by the Bay of Stoer Formation and unconformably overlain by the Applecross

134 Formation. At Rubha Réidh, the succession is truncated to 100 m thickness, with a faulted lower

135 contact and the Diabaig Formation unconformably overlain above (Stewart, 2002). FA1 consists

136 nearly entirely of sandstone (>99% of total strata). Mudstones (<1%) are restricted to mm-

137 thick, often desiccated, laterally discontinuous layers or intraformational mud clasts.

138 Sandstones are medium-grained, with the exception of the lowest 7 m of stratigraphy at Stoer,

139 where pebbly sandstones occur. Lower bounding surfaces are either flat (Fig. 3B), or drape and

140 preserve an underlying dune topography (Fig. 3C). Erosion between sand-bodies is restricted to

141 localized scours, no more than 50 cm deep. Various stratification types and bedding plane

142 features are present (Table 1). Three-dimensional outcrops permit the identification of both

143 foreset and backset (cross-stratification dipping up local palaeoflow) stratification and foreset

144 dips indicate that palaeoflow was towards 279° (n = 41). The description and interpretation of

145 each stratification type and bedding plane feature are as follows.

146 **3.1.1. Sandstone stratification types**

147 Stratification types in this section are documented in order of progressively decreasing

148 associated flow strength: their relative frequency of occurrence is shown in Figure 2.

149 **3.1.1a. Backset laminae associated with an upstream-dipping scour surface** *(Chute and*

150 *Pool structures)*

151 *Description* – Asymmetric scoured surfaces, filled by upstream-inclined cross laminae are

152 present at Rubha Réidh and Stoer (Fig. 4). Backsets truncate against steep, downstream-dipping

153 scoured margins, and are succeeded vertically by horizontal laminations and convex-up

154 bedding. At Stoer, convex-up bedding passes down-flow into horizontal laminations with soft-

155 sediment deformation structures (Fig. 4B).

156 *Interpretation* – Comparable features are rarely reported from the rock record (Fralick, 1999;

157 Fielding, 2006; Lowe and Arnott, 2016; Winston, 2016), but are analogous to chute and pool

158 structures formed in laboratory experiments (Alexander et al., 2001; Cartigny et al., 2014).

159   Chute and pool structures form due to a temporary hydraulic jump within a localized scour

160   when shallow, faster flowing waters (the chute) pass immediately into deeper, slower flowing

161   waters (the pool) (Fielding, 2006). Their relationship with juxtaposed bedforms in the MDF

162   indicate that the pools were filled prior to flow waning to regimes associated with the

163   deposition of antidune stratification and horizontal laminations. High-velocity and turbulent

164   flow conditions account for the association of chute and pool structures with soft-sediment

165   deformation.

166   **3.1.1b. Convex-up bedding containing backset cross-laminae** *(Antidunes)*

167   *Description* – Convex-up bedding is occasionally associated with otherwise horizontal beds (Fig.

168   5). Convex-up beds are low-relief (20 – 25 cm), symmetrical and internally characterized by

169   cross-laminae that dip upstream (compared to palaeocurrents from nearby dune cross-

170   stratification). They are solitary and do not form larger concavo-convex sets. Widths of convex-

171   up portions range from 200 – 225 cm.

172   *Interpretation* – Symmetrical, convex-up beds with internal upflow-dipping cross-laminae

173   suggest that they formed in the antidune stability field (e.g., Fielding, 2006; Cartigny et al.,

174   2014). Antidune stratification has been produced in experimental flows underneath transient

175   standing waves (e.g., Kennedy, 1963; Alexander et al., 2001), suggesting that standing waves

176   developed in supercritical flow conditions during the deposition of the MDF. Their comparative

177   scarcity compared with horizontal laminations (section 3.1.1c) reflects the transient nature of

178   such flow conditions and the relatively low preservation potential of antidune stratification.

179   Additionally, confident diagnosis of antidune stratification requires full preservation of the

180   bedform under aggrading sedimentation (Cartigny et al., 2014), meaning that the number of

181   identifiable antidune deposits in the MDF is likely an under-representation of their true

182   abundance.

183   **3.1.1c. Horizontal laminations** *(Upper plane bed)*

184 *Description* – Horizontal laminations constitute the basal parts of the majority of FA1 sand-

185 bodies (>95%) (Fig. 6; Fig. 8). Thin (< 4 mm), ungraded laminae occur in sets 5 – 110 cm thick.

186 Sets are tabular in depositional-dip and strike sections. Underlying bounding surfaces are flat

187 and exhibit no evidence of incision into the underlying bed (at outcrop scale). In large

188 depositional-dip outcrops, planar laminations occasionally transition laterally to low-angle,

189 down-flow dipping cross-stratification (section 3.1.1e).

190 *Interpretation* – Horizontal laminations record upper-flow regime plane bedding (Paola et al.,

191 1989). Upward transitions from upper- to transitional upper-flow regime sedimentary

192 structures are interpreted as the product of waning floods. Similarly, down depositional-dip

193 transitions from horizontal laminations to low-angle cross stratification represent lateral

194 decreases in flow strength (upper- to transitional upper-flow) (Fielding, 2006).

195 **3.1.1d. Asymmetrical sigmoidal sets of cross-stratification** *(Humpback dunes)*

196 *Description* – Cross stratification exhibiting a downflow-divergent sigmoidal geometry is

197 present in multiple sand-bodies at Rubha Réidh (Fig. 6; Fig. 7A). The sigmoidal geometry

198 permits the differentiation of discrete topset, foreset and bottomset elements. Convex-up bed

199 topography is apparent at the top of each set (Fig. 7A); a stratification type referred to as

200 humpback cross-stratification (Saunderson and Lockett, 1983; Fielding, 2006). Sets are up to

201 2.2 m high and can be traced down depositional-dip for > 65 m (Fig. 6). Ripple marks are

202 frequently preserved in topographic lows associated with preserved convex-up topography

203 (Fig. 6). In three-dimensional sections, it is clear that humpback sets comprise wedge-shaped

204 packages that built out in a westwards direction (Fig. 7B).

205 *Interpretation* – Humpback 'form-sets' develop when deposition dominates over erosion at flow

206 conditions transitional between the dune stability field and the upper plane bed field

207 (Saunderson and Lockett, 1983). Convex-up bed topography at the top of each set implies that

208 the bedforms are fully preserved ('form-sets') (Reesink et al., 2015).

209 **3.1.1e. Low-angle (<20°) cross-stratification** *(Transitional upper-flow regime dunes)*

210 *Description* – Low angle cross-stratification occurs throughout the MDF (Fig. 8A). Foreset dip

211 angles range from 5° - 15°. In depositional-dip sections, low-angle foresets occasionally merge

212 into horizontal laminations up-flow.

213 *Interpretation* – Low-angle cross-stratification develop at flow conditions transitional between

214 dune stability field and upper plane bed stability (Fielding, 2006). Lateral transitions between

215 horizontal laminations and low-angle cross stratification reflect localized variations in flow

216 energy.

217 **3.1.1f. High-angle (>20°) cross-stratification** *(Lower flow-regime dunes)*

218 *Description* – Planar cross-stratification occurs in solitary sets of 10 - 30 cm thickness. Co-sets of

219 planar cross-stratification do not occur; instead, sets are intercalated with sedimentary

220 structures associated with upper-flow regime flows (most abundantly horizontal laminations)

221 (Fig. 8B). Sets are highly tabular and show minimal lateral thickness changes in both

222 depositional-dip and depositional-strike sections. Trough cross-stratification was only observed

223 at the base of the formation at Stoer (coincident with the only pebbly interval observed in the

224 MDF).

225 At Rubha Réidh, in instances where cross-bedded units occur at the top of a major sand-body,

226 dune topography is preserved (Fig. 2; Fig. 3A; Fig. 9A). Dunes are spaced 0.5 - 1 .5 m apart and

227 have heights of 10 - 30 cm. Abundant ripple marks are superimposed onto the dune

228 microtopography (section 3.1.2a).

229 *Interpretation* – The migration of lower-flow regime two- and three-dimensional subaqueous

230 dunes produce planar and trough cross beds respectively. The existence of tabular sets with

231 minimal lateral variation in relief implies that flow depths were consistent across large areas.

232 Co-sets of high-angle cross-stratification are entirely absent, with cross-stratification most

233   commonly occurring between upper-flow regime sedimentary structures suggesting their

234   deposition relates to waning high-energy floods.

235   **3.1.2. Bedding plane features**

236   In the MDF, ripple marks and other sedimentary surface textures are common on some bedding

237   surfaces, which record the preservation of primary substrates. Sedimentary surface textures

238   exhibit a wide variety of morphologies, due to their formation on substrates that persisted for

239   variable intervals of sedimentary stasis (Davies et al., 2017b). This morphological variability

240   may hamper the determination of whether the textures had a microbial or abiotic origin, so in

241   this section they are classified following the technique described in Davies et al., (2016):

242   Category A structures are demonstrably abiotic in origin; Category Ba is used where

243   circumstantial evidence suggests structures may be biotic, but an abiotic origin cannot be ruled

244   out; Category Ab is used for the opposite situation to this; Category ab is used where there is no

245   clear evidence to support abiotic or biotic origin.

246   **3.1.2a Ripple-Marks**

247   *Description* – Symmetrical ripple-marks are nearly ubiquitous on each studied planform surface

248   (n = 12) at Rubha Réidh, Balchladich Bay and Stoer (Fig. 9). The largest of these exposed

249   surfaces has an area of >1000 m^2. Ripple-marks are frequently seen superimposed on top of

250   dune topography, where they have weakly anastomosing sinuous crests which rarely extend > 2

251   m (Fig. 9A). On flat surfaces which lack dune microtopography, crests are subparallel and

252   extend for > 10 m (Fig. 9B). Ripple-marks record unidirectional flow on individual bedding

253   planes, but a near 360° dispersal is apparent when all rippled surfaces are considered (Fig. 9B).

254   The modal E-W strike-line is perpendicular to the prevailing westward flow ($\theta = 279°$; n = 41).

255   Many ripple marks have clear drainage lines etched into their flanks, indicating emergence and

256   drainage subsequent to their formation (Fig. 10A, 10B). Crests are mostly well-rounded or flat-

257   topped. Sharp crested ripple marks are rare (Fig. 10C), and contain synaeresis cracks within

258   their troughs (Fig. 10D). Infrequent interference ripple-marks occur (Fig. 10E). Ripple-marks

259   located within dune troughs are often draped by mud (Fig. 10F).

260   In addition to planform exposures of ripple-marks, trains of ripple crests can be observed

261   within vertical sections (Fig. 6; Fig. 10G). Above humpback dunes, sharp crested ripple-marks

262   are present in dune troughs and form ripple trains which extend laterally for up to 4 m (Fig. 6).

263   In rare instances ripple crests display uneven oversteepening (Fig. 10H).

264   *Interpretation* – Symmetrical ripple-marks record bedform stability under low flow regime:

265   representing falling flood stage. Their near-ubiquitous positioning above sand-bodies that

266   contain upper- and transitional-upper flow regime sedimentary structures suggests that flood

267   waters receded to leave pools of standing water across the depositional plain. Their

268   comparatively greater abundance within humpback dune troughs (compared with crests) lends

269   further credence to this notion, suggesting more pervasive pooling of water within pre-existing

270   topographic lows. Variations in ripple-crest strike-line suggest that this ponded water drained

271   and moved in different directions, depending on localized slope and wind conditions. Soft

272   sediment deformation of some ripple crests may have been caused by current drag over the

273   rippled surface during subsequent flooding events. Alternatively the oversteepening may be

274   seismically induced.

275   **3.1.2b Adhesion Marks (A)**

276   *Description* – Adhesion marks are frequently seen to be superimposed upon ripple-marked

277   surfaces (Fig. 11). They present as 2 – 5 mm wide, 1 – 3 mm high positive epirelief mounds that

278   are irregular in form (i.e., adhesion marks and not adhesion ripples; Kocurek and Fielder, 1982).

279   Their spatial distribution across any given bedding surface is strongly dependent on the

280   associated dune and ripple microtopography (Fig. 11). On dune crests (topographic highs),

281   ripple-marks are densely blanketed by adhesion marks across their crests and troughs (Fig.

282   11A). Within dune troughs (topographic lows), adhesion marks are only ever restricted to

283   ripple crests, or are absent entirely (Fig. 11B). On flat beds lacking dune microtopography,

284   adhesion marks occur on both ripple crests and troughs, but are more common on the former

285   (Fig. 11C).

286   *Interpretation* – Adhesion marks indicate that water-lain sands were intermittently subaerially-

287   exposed, permitting the accretion of wind-blown sand grains onto moist substrates (Kocurek

288   and Fielder, 1982). Adhesion marks are progressively more common with height above the

289   surface (i.e., most common on ripple crests on dune crests; least common in ripple troughs in

290   dune troughs), indicating that they can be used to locally determine how extensive the recession

291   of pooled water was between flood events. The total absence of adhesion marks in some dune

292   troughs suggests that, in some instances, no subaerial exposure occurred and that pooled water

293   persisted until the subsequent flood event (Fig. 11A-C).

294   **3.1.2c Sinuous shrinkage cracks (*Manchuriophycus*) (Ba)**

295   *Description* – Sinuous shrinkage cracks were observed at one ripple-marked surface at Rubha

296   Réidh. Cracks are up to 1 cm wide and 25 cm long. They most commonly occur within, and

297   parallel to, ripple troughs, but individual cracks may also cross ripple crests (Fig. 12). They are

298   preserved in positive epirelief, although post-depositional erosion often results in

299   accompanying negative epirelief impressions.

300   *Interpretation* – The sinuous shrinkage cracks fit the type description of the "pseudofossil"

301   *Manchuriophycus* (Endo, 1933). *Manchuriophycus* has variously been interpreted as fossilized

302   algae, a burrow structure, or inorganic desiccation crack (see Hantzschel, 1962); though is now

303   more commonly thought a type of microbially-induced sedimentary structure (*sensu* Noffke et

304   al., 2001) arising due to the shrinkage of microbial mats with very high strengths and elasticity

305   (Koehn et al., 2014). In the absence of a mat, grains would more likely have accommodated

306   stress by moving past one another rather than opening cracks (McMahon et al., 2016). If the

307   MDF examples have a microbial origin, their preferential development in ripple troughs would

308   imply that matgrounds were thicker within topographic lows (Schieber, 2007).

309   Prave (2002) reported similar features ('irregular- to rod-shaped fragments of variable length

310   and curvature concentrated within ripple troughs', p. 813) and interpreted these as fragments

311   of microbially bound sand layers that had been entrained and rolled during ephemeral flows

312   (his Fig. 4A). Surfaces with well-formed *Manchuriophycus* identified during this study also host

313   positive epirelief fragments similar in morphology to the fragments described by Prave (2002)

314   (Fig. 12).

315   **3.1.2d Reticulate Markings (Ba)**

316   *Description* – Reticulate ridges occur on multiple planform surfaces (Fig. 13A; Fig. 13B).

317   Individual nets are 2 – 6 mm wide and 1 – 2 mm high.

318   *Interpretation* – Reticulate markings have modern analogues in cyanobacteria and eukaryotic

319   algae, where they arise from filament tangling (Shepard and Sumner, 2010; Davies et al., 2016).

320   **3.1.2e Serrated margins (ab)**

321   *Description* – In rare instances, clear serrated margins several millimeters thick separate

322   bedding plane surfaces with and without adhesion marks (Fig. 13C).

323   *Interpretation* – Prave (2002) interpreted the serrated margins as remnants of microbially

324   bound layers, where sand grains had adhered to a microbial crust (due to the presence of sticky

325   extracellular polymeric substances and cyanobacterial filaments). Possible alternative abiotic

326   explanations for the margins could include: (1) post-depositional partial erosion of overlying

327   sediment layers; or (2) original patchy distribution of moist sands resulting in localized

328   adhesion.

329   **3.1.2f Desiccated Sandstone (ab)**

330   *Description* – In rare instances, desiccated polygons overprint ripple marks without a muddy

331   matrix (Fig. 14A). Polygons are 15 - 25 cm wide and a few centimeters deep.

332   *Interpretation* – Desiccation cracks only develop in materials with sufficient cohesive strength

333   (e.g., van Mechelen, 2004). Within moist (abiotic) sands, such cohesion can only be attained if

334   grains have high textural maturity (Chavdarian and Sumner, 2011; Glumac et al., 2011). To date,

335   desiccation experiments on clay-poor sand substrates with angular grains have been

336   unsuccessful (Kovalchuk et al., 2016). However, microbiota can increase sand cohesion by

337   stabilizing grains with cyanobacterial filaments and extracellular polymeric substances (e.g., De

338   Bore, 1981) and, in doing so, enable polygon formation (Prave, 2002; Eriksson et al., 2007;

339   Kovalchuk et al., 2016; McMahon et al., 2016). Whilst this is a viable formation mechanism, the

340   absence of proximal microbial fabrics on the desiccated sandstone bed at Rubha Réidh means

341   that no direct evidence for a microbial origin has been conclusively ascertained in this study.

342   **3.1.3 Desiccated Mudstone**

343   *Description* – The mudstones that account for <1% of FA1 are ubiquitously desiccated, with

344   individual polygons up to 1 m in diameter (Fig. 14B).

345   *Interpretation* – Desiccated mudstones result from a reduction in volume as muds dry out when

346   emerged (Bradley, 1933), indicating that all the preserved Meall Dearg mudstones were

347   deposited immediately prior to subaerial exposure.

348   **3.1.4 Interpretation of Facies Association 1** *(High energy alluvial events)*

349   Sand-bodies at Stoer, Rubha Réidh and Balchladich Bay are interpreted as the deposits of

350   multiple high-energy alluvial flood events. During peak flow, upper-flow regime conditions

351   prevailed (Fielding, 2006), occasionally entering the chute and pool or antidune stability

352   regimes (Alexander et al., 2001; Cartigny et al., 2014). As floods waned, flows progressively

353   operated under transitional upper- and subcritical flow-conditions, resulting in the vertical

354   stacking of sedimentary structures in accordance to decreasing flow velocity (Fig. 2). At Stoer,

355   stratification types are typically limited to intercalated horizontal laminations and planar cross-

356   stratification, with each package the result of an individual flood. Packages at Stoer are rarely

357 greater than 20 cm thick, implying either shallow flow depths or partial erosion by successive

358 flood events. This is in contrast to the variety of preserved stratification at Rubha Réidh, where

359 humpback form-sets are up to 2.2 m thick and must have been submerged in deeper water

360 during deposition. During high flood stages, it is implicit that the critical flow velocity for

361 coarse-sediment transport was exceeded, so the absence of such sediment grades indicates

362 either: (1) only medium-grained sediment in the primary sediment supply (e.g., due to a

363 significant distance from the sediment source); or (2) bypass of coarser sediment fractions.

364 Variably-striking ripple crestlines are superimposed on nearly all studied sand-bodies reflecting

365 unconfined post-flood pooling of quiescent waters.

366 Abundant adhesion marks and desiccation cracks indicate intermittent subaerial exposure. The

367 diversity of reticulate markings, *Manchuriophycus*, and other surface textures with ambiguous

368 origin, offer strong circumstantial evidence for microbial colonization of substrates during

369 sedimentary stasis (Schieber, 1999; Prave, 2002; Davies et al., 2016).

370 No apparent unconformity exists between the MDF and the underlying Bay of Stoer Formation,

371 but the boundary marks a major change in sedimentary lithofacies. Bay of Stoer Formation

372 fluvial facies consist of stacked, lower flow-regime, three-dimensional sedimentary structures

373 (Stewart, 2002; Ielpi et al., 2016), typical of perennial fluvial flow (Bristow, 1987; Best et al.,

374 2003), and are overlain by the shallow lacustrine Poll a'Mhuilt Member (Stewart, 2002). In

375 contrast, MDF deposition occurred as high energy events; a lithofacies shift that probably

376 reflects changes in the regional temperature and seasonality of precipitation (e.g., Fielding,

377 2006; Lowe and Arnott, 2016), within the low-latitude, semi-arid climate belt where the

378 formation was deposited (Torsvik and Sturt, 1987; Stewart, 1990). Alternatively, the

379 stratigraphic appearance of these features may be a preservational artefact related to changes

380 in basin accommodation, but, as the duration of hiatus at the Poll a' Mhuilt-Meall Dearg

381 boundary is not understood, such a control cannot be confidently assessed.

382

3.2. Facies Association 2 *(Enard Bay)*

The 150-250 m thick MDF succession at Enard Bay overlies the Poll a' Mhuilt Member (not exposed in continuous coastal section) and is unconformably overlain by the Diabaig Formation (Stewart, 2002). Due to lithofacies dissimilarity, Gracie and Stewart (1967) and Stewart (2002) did not correlate these strata with those described in Section 3.1., but the locality is now the British Geological Survey reference section for the MDF (BGS Lexicon of Named Rock Units [online] accessed 2017). Here, the Enard Bay strata are recorded as Facies Association 2. FA2 deposits are near-ubiquitously composed of fine- or medium-grained sandstones (Fig. 2; Fig. 15A; Fig. 17B). No mudstones were observed in this study. Planar cross-beds occur in sets 1 – 5 m thick, intercalated with laterally extensive planar beds up to 2.8 m thick (Fig. 15A; Fig. 15B). These sedimentary characteristics indicate an aeolian origin for FA2, which was likely deposited coevally to the FA1 alluvial deposits. Although an aeolian interpretation was previously discarded by Stewart (2002) on the basis that 'convex upward aeolian reactivation surfaces comparable in size with those figured by McKee (1967) were not observed' (p. 72), an absence of such features is not diagnostic proof against aeolian deposition. Two sedimentary facies are described, in support of an aeolian origin: [1] Large-scale planar cross-bedded; and [2] Planar-bedded. These facies are exclusive of the southernmost outcrop currently mapped as MDF; a singular exposure of occasionally pebbly, coarse-grained, cross-bedded sandstone separated from the described succession by 250 m (Krabbendam, 2012). This c. 5 metre-high and c. 30 metre-wide partially exposed outcrop forms a prominent small knoll, apparently faulted into contact with the rest of the MDF at Enard Bay (Fig. 16). Given the dissimilarity of its facies to the remainder of the succession, the inability to confirm a genetic relationship with the rest of the MDF strata at Enard Bay, and the local presence of faulted slivers of pebbly sandstones of the Applecross Formation, the exposure is here considered most likely to be a previously unrecognized outcrop of the latter formation. However, even if the outcrop records a basal pebbly fluvial facies with the remainder of the local MDF, this lithology is never seen to be interbedded with the overlying aeolian facies.

3.2.1 Large-scale planar cross-bedded sandstones *(Aeolian dunes)*

Description – Large-scale planar cross-bedding occurs within fine- to medium-grained well-rounded arkosic arenites. Cross-beds occur in sets of 1.2 – 5 m thickness (Fig. 15A), which are planar in depositional-dip sections (Fig. 15B) and curved in depositional-strike sections (Fig. 15C). Curved foresets demonstrate palaeoflow spreads of up to 40° across individual sets (Fig. 15D, Fig. 15E), although the dispersal does not detract from the highly-unimodal WSW-directed stacking of dune foresets (θ = 248°, n = 201). Individual sets are up to 40 m wide, with typical angles of climb between 15 – 25° (maximum 34°). Individual foresets are characterized by 1 – 4 mm thick, steeply dipping cross laminae with subtle inverse grading (Fig. 17A) or planar laminae with no discernible grain-size trends (Fig. 17B). Cross-bedded sets are typically bound by planar bedded sandstones (see Section 3.2.2; Fig. 15A; Fig. 15B). When planar-beds are absent, dune sets are separated by low-angle, erosional reactivation surfaces (Fig. 18A).

Interpretation – The presence of fine- to medium-grained sandstones with well-rounded grains, arranged in cross-strata sets that are composed of cross-laminae (grainflow) and planar laminae (grainfall) suggests that the planar cross-bedded facies represent aeolian dune deposits (e.g., Hunter, 1977; Kocurek, 1981, 1996). High dispersal of palaeoflow measurements across individual dune sets, and curved crest lines (Fig. 15C) suggest that the dunes were arcuate.

3.2.2 Planar-bedded sandstones *(Aeolian interdunes)*

Description – Planar-bedding occurs in packages of fine- and subordinate medium-grained arkosic arenites, 0.1 – 2.4 m thick, and display near ubiquitous pin-stripe lamination (Fig. 17D). Adhesion lamination is uncommon (Fig. 17E). Planform surfaces are largely featureless, but sometimes contain adhesion marks (Fig. 17F) or, rarely, poorly developed ripple marks (n = 4) exhibiting a near 90° spread of strike lines.

Within the planar-bedded facies, one known example of a coarse-grained, apparently massive channelized sand-body incises into a 2.4 m thick planar-bedded package (Fig. 18B). Exposure

435   constraints restrict full dimensions from being determined, but the preserved sand-body is at

436   least 9 m wide and has a relief of 1.5 m.

437   *Interpretation* – Planar-bedded facies are interpreted as aeolian interdunes. Pin-stripe

438   lamination and climbing ripple stratification can form by aeolian ripple migration under

439   aggrading conditions (Fryberger et al., 1988; Hunter, 1977). Adhesion marks record moist

440   interdune surfaces. The interpreted interdune packages are comparatively thinner

441   (predominantly <1 m, maximum 2.4 m) and less laterally extensive than dune surfaces. The

442   channelized sand-body may be (the only) evidence for fluvial deposition in FA2, but the absence

443   of internal structure forbids further interpretation. If fluvial in origin, it differs from the FA1

444   alluvium at Rubha Réidh, Balchladich Bay and Stoer through its coarser grain size and presence

445   of channel margins.

446   **3.3. Mutual exclusion of aeolian and fluvial deposits**

447   The mutual geographic exclusion of the aeolian facies association at Enard Bay (FA2) and fluvial

448   facies association at Rubha Réidh, Balchladich Bay and Stoer (FA1) is not unexpected. In many

449   modern mixed fluvial-aeolian systems, there is a high propensity for fluvial flood-reworking of

450   neighbouring aeolian dune deposits (e.g., Kocurek and Nielsen, 1986; Langford, 1989), biasing

451   the resultant sedimentary record towards alluvial dominance. This preservation bias may have

452   been particularly acute in pre-vegetation systems, when plant-related factors that can buffer

453   against reworking (such as sediment binding and baffling by roots, and the reduction of near-

454   surface flow velocities by above-ground structures) were absent (Tirsgaard and Øxnevad, 1998;

455   Rodriquez et al., 2014). Furthermore, wind-blown sands may have been more readily deflated

456   from the alluvial realm in the absence of vegetation (Dalrymple et al., 1985; Lancaster and Baas,

457   1998; Mountney, 2004). Deflation may also have been locally promoted by a low groundwater

458   table (as suggested by the absence of wet interdune facies in the MDF) (Fryberger et al., 1988;

459   Kocurek and Havhom, 1993; Tirsgaard and Øxnevad, 1998). In such a scenario, the aeolian

460   strata at Enard Bay would represent exceptional preservation of deposits that were originally

461 more common when the MDF depositional environments were active; their absence at Rubha

462 Réidh, Balchladich Bay and Stoer reflecting the biasing effects of high-energy flood events. The

463 limited outcrop of the MDF at Enard Bay does not permit a robust explanation for their

464 exceptional preservation to be determined, but any one of a number of potential preservation

465 mechanisms may have been responsible (e.g., relating to climate, sediment supply, rate of dune

466 migration or accommodation space generation; Mountney, 2012).

467 **4. DISCUSSION**

468 **4.1. Architectural analysis in outcrop of limited exposure**

469 Where extensive along-strike and down-dip exposure of alluvial strata exists, architectural-

470 element analysis (e.g., Miall, 1985; Long, 2011) can be a powerful conceptual tool for elucidating

471 geomorphic and planform components of pre-vegetation river systems (e.g., Long, 2006; Ielpi

472 and Rainbird, 2015). However, such outcrop quality is not universal to all pre-vegetation

473 alluvial successions. The MDF provides a useful case-study in the importance of taking a

474 conservative approach by making interpretations of alluvial strata based only on observable

475 geological phenomena in the field. The formation contains sufficient primary sedimentary

476 geological signatures to conclusively affirm its deposition by high-energy floods, but its outcrop

477 quality and accessibility is unsuited for any robust interpretation of fluvial planform. In this

478 discussion, we emphasise (1) that the outcrop quality of the MDF is not unusual for strata of

479 Mesoproterozoic age and that the use of succession-scale architectural analysis on this unit, or

480 similarly-exposed units, is inappropriate; and (2) in instances such as this, the term "sheet-

481 braided" (used in inverted commas, and only when diagnostically-applicable) is useful

482 descriptive nomenclature, confirming the distinct nature of pre-vegetation alluvium.

483 **4.1.a. Limitations of determining alluvial architectural style in the Meall Dearg Formation**

484 The MDF is unsuited for succession-scale architectural analysis due to the nature of its outcrop.

485 Its maximum along-strike exposure is 50 metres at Enard Bay and 140 metres at Stoer. These

486 maximum exposures are dissected by multiple local faults and joints, rendering it rarely

487 possible to trace stratigraphic bounding surfaces along their original extent. Large-scale

488 depositional architectures are unsuited for interpretation from satellite imagery, as has been

489 undertaken for older units of the Stoer Group (Ielpi et al., 2016), for three reasons: (1) The

490 strata are tectonically inclined between 25-30° and have a NNE strike (Fig. 19A). Vertical

491 observation of beds that crop out obliquely in plan-view greatly exaggerates true bed thickness

492 and means that successive bounding surfaces are laterally offset; (2) Coastal exposure

493 disappears underneath a variably deep cover of post-glacial till and peat bog within metres east

494 of the coast (Fig. 19B). Topographic mapping cannot trace beds beneath this drift as its relief is

495 not influenced by the depositional stratigraphic architecture of the underlying, lithologically

496 homogenous formation; (3) Key stratigraphic contacts are variably obscured by local jointing,

497 weathering, beach debris, vegetation, and intertidal algae. We deliberately refrain from making

498 any inference of ancient fluvial planform for the MDF as any such 'interpretation' would be

499 speculative and methodologically distinct from the robust interpretation of high-energy flood

500 deposition, made from primary field observation.

501 **4.1.b. "Sheet-braided" fluvial style: a polygenetic architectural signal of Precambrian**

502 **alluvium**

503 While the outcrop quality of the MDF prohibits a refined architectural assessment of the unit,

504 the exposure is still of sufficient quality to recognize that its constituent alluvial sandbodies

505 exhibit an almost uniform "sheet-braided" architecture (*sensu* Cotter, 1978). The term "sheet-

506 braided" was introduced by Cotter (1978) for individual genetic units of sandstone with

507 width:depth ratios greater than 20:1. His original definition explicitly stated that "sheet-

508 braided" was a subdivisional classification of the 'fluvial style' of an alluvial sedimentary

509 package (Cotter, 1978, p. 364), and that 'fluvial style' referred to the character of an alluvial *rock*

510 *sequence* (Cotter, 1978, p. 362), independent of any conceptual models of fluvial planform for

511 the depositional environment of a given unit. This strict definition of the term was maintained

512 in the three decades after Cotter's (1978) work, and was reiterated by Davies & Gibling (2010)

513 and Davies et al. (2011). Recently, however, the term has increasingly become conflated as

514 having geomorphological significance for original fluvial planform, and a number of papers have

referred to 'sheet-braided rivers' (e.g., Ielpi and Ghinassi, 2015; Ielpi and Rainbird, 2016b; de Almeida et al., 2016). The inclusion of the word 'braided' in Cotter's (1978) term is thus unfortunate, due to the confusion between geomorphology and sedimentology that has subsequently arisen.

In response to this conflation of geomorphological form and sedimentary product, a number of papers have argued against the predominance of "sheet-braided" Precambrian alluvium, on the basis that special circumstances of outcrop and exposure may permit a more refined interpretation of fluvial planform during deposition (e.g., Ielpi and Rainbird, 2015, 2016a,b; Santos and Owen, 2016). However, even when such interpretations are possible, most examples of Precambrian alluvium remain "sheet-braided" *sensu* Cotter (1978) (e.g., minimum 30:1 aspect ratio foreset bar sandbodies; Ielpi and Rainbird, 2016b; 20:1 to 80:1 channel sandbodies; Ielpi and Ghinassi, 2015). Such "sheet-braided" fluvial style is clearly polygenetic: applying the original definition, examples are known where the architecture has developed deposited by highly mobile channels (e.g., Todd and Went, 1991; Rainbird, 1992; McMahon et al., 2017), exceptionally wide channels (e.g., Fuller, 1985; Nicholson, 1993), deep channelled drainage (Ielpi and Rainbird, 2016b; Ielpi et al., 2016), unconfined flow (e.g., Winston, 2016) and high-energy flood events (Tirsgaard and Øxnevad, 1998; this study).

Despite these issues, we contend that the term still has value, providing that it is used as a passive descriptor of architectural properties rather than carrying implications of palaeoenvironmental setting. The first factor in support of the retention of the term is that in many natural geological outcrops, such as those of the MDF, the low diagnostic bar for the identification of "sheet-braided" architecture (>20:1 aspect ratio) means that this architectural characteristic can still be identified or rejected, even when more refined architectural interpretation is prohibited. The second factor in support of its retention is that the characteristic retains importance as a key distinction between alluvium deposited before and after the evolution of land plants: the ubiquity of "sheet-braided" alluvium in Precambrian strata means that it may be mistakenly perceived as a bucket term, but its true merit lies in the

542 converse fact that there are no known examples of post-Silurian alluvial successions that are

543 dominated by such architecture. Thus, in a holistic view of alluvium through time, the

544 Precambrian dominance and Phanerozoic diminishment of "sheet-braided" alluvium attests to

545 the significance of the evolution of a terrestrial flora in promoting a wider diversity of preserved

546 alluvial phenomena.

547 In order to maintain these clear practical and conceptual uses, we propose that the term "sheet-

548 braided" should continue to be applied in studies of ancient alluvium, but that it should be used

549 in inverted commas in future studies, in recognition of the fact that the term is applicable to a

550 variety of polygenetic alluvial strata and is not necessarily diagnostic of a braided fluvial

551 planform at the time of deposition. Despite the potentially confusing inclusion of the word

552 'braided' in the term, its continued usage is preferential to the adoption of new terminology

553 because: (1) the term "sheet-braided" is already entrenched in published literature; (2) any new

554 terminology would require reference to the 'sheet' form of the strata, but sedimentological

555 terminology invoking this term is already congested and requires careful application (North &

556 Davison, 2012); and (3) the inherent fuzziness of the rock record, the vagaries of outcrop

557 exposure and preservation, and the need for revision of concepts as new observations are made,

558 mean that the science of sedimentary geology is necessarily pragmatic in its terminology: there

559 is strong precedent for the retention of terms that no longer carry the implicit interpretation

560 apparent in their wording (e.g., synaeresis cracks (McMahon et al., 2016), the sedimentary

561 structure 'Kinneyia' (Davies et al., 2016), various ichnological and ichnofacies terms (Minter et

562 al., 2016)). We emphasise that the term should always be used in conjunction with more

563 detailed analysis when outcrop quality permits and that it is not exclusive of other, more refined

564 classification schemes (e.g., Krynine, 1948; Friend et al., 1979, Friend, 1984; Gibling, 2006).

565 Improved adoption of the term "sheet-braided" in its original sense (Cotter, 1978) will promote

566 the comparability of different studies, paving the way for a better understanding of the truly

567 unique characteristics of pre-vegetation alluvium and the Palaeozoic transition away from

568 "sheet-braided" ubiquity. A better understanding of the global and stratigraphic distribution of

569   "sheet-braided" alluvium will potentially shed light on the extrinsic factors that determined why

570   this *fluvial style* was apparently such a common geological signature of a variety of different pre-

571   vegetation *fluvial systems*.

572

573   **4.2. Aggradation and stasis during deposition permit the identification of high-energy**

574   **flood events**

575

576   Preserved Meall Dearg stratification types and sedimentary surface textures have enabled the

577   identification of high-energy flood events, but this interpretation was only permitted because

578   the strata contain direct evidence for: (1) upper-flow regime bedforms deposited by rapidly

579   decelerating flows under highly aggrading bed conditions; and (2) bedding plane records of

580   intervals of sedimentary stasis.

581   Upper-flow regime bedforms such as antidunes have traditionally been considered to be

582   transient sedimentary features, with limited long-term preservation potential (e.g., Reid &

583   Frostick, 1994). However, they can be preserved, unmodified, when the rate of deceleration

584   does not permit bedforms to equilibrate with flow regime (McKee et al., 1967; Alexander and

585   Fielding, 1997; Alexander et al., 2001); conditions that may have been more frequent during

586   Earth history than has traditionally been assumed (Fielding, 2006). The stacking of stratification

587   types recording progressively lower-flow regime conditions, as can be seen in the MDF, is

588   attributable to such conditions of rapid sediment fall-out during falling flood stages. The

589   preservation of these signatures, in addition to the full preservation of convex lamina sets

590   within antidunes, attests to high rates of bed aggradation during sedimentation (Alexander and

591   Fielding, 1997; Fielding, 2006; Cartigny et al., 2014).

592   The exceptional aggradational preservation of antidunes and related bedforms provides direct

593   evidence that supercritical flow conditions developed during alluvial deposition, but cannot

594   determine whether such conditions were perennial or whether they instead reflect discrete

595 high-energy flood events. The determination of event deposition requires separate evidence

596 that the sedimentary system repeatedly reverted to background conditions of low flow regime

597 or sedimentary stasis (neither deposition nor erosion; Tipper, 2015) subsequent to the

598 development of supercritical flow. In the MDF, the packages of sediment revealing supercritical

599 flow are sandwiched between strata that preserve bedding plane evidence for prolonged

600 intervals of sedimentary stasis. Such features include sedimentary surface textures of both

601 abiotic (adhesion marks and desiccation cracks) and likely microbial origin (e.g., reticulate

602 marks, *Manchuriophycus*), analogous to modern features that develop during sedimentary stasis

603 in ephemeral streams (Davies et al., 2017b). In order for such original substrate features to have

604 become preserved in the sedimentary record, the succeeding flows must have lacked the

605 capacity to erode the underlying substrate. In sparsely-vegetated modern and ancient

606 ephemeral alluvial settings, rapidly aggraded sediment piles can change the locus of subsequent

607 sedimentary events, thus escaping erosional truncation (Field, 2001; Cain and Mountney, 2009).

608 In the MDF, evidence for such conditions can be seen in the way in which bounding surfaces are

609 rarely erosional; succeeding packages of strata, most often floored with upper-flow regime

610 elements, are deposited directly above preserved topography (Fig. 3). This indicates that,

611 despite the surpassing of a critical threshold for the deposition of upper flow bedforms, the

612 critical threshold for erosion of underlying strata was not exceeded. The only erosional contacts

613 in the entire succession are restricted to laterally discontinuous <50 cm scour-cuts. These

614 characteristics of the MDF suggest that highly aggrading bed conditions can enhance the

615 preservation potential of strata recording sedimentary stasis, in addition to supercritical

616 bedforms.

617 **5. CONCLUSION**

618 The spatial distribution of stratification types and bedding plane features across the

619 Mesoproterozoic Meall Dearg Formation indicate deposition by high energy alluvial events and,

620 subordinately, as aeolian dunes. The alluvial and aeolian sedimentary facies are mutually

621 exclusive: potentially suggesting aeolian sediments were only preserved in regions less prone to

622 reworking by alluvial activity. The "sheet-braided" alluvial sandstones contain a variety of

623 stratification types relating to upper-flow (chute and pool structures, antidune stratification,

624 horizontal laminations), transitional upper-flow (humpback cross-stratification, low-angle cross

625 stratification) and lower flow-regime conditions (planar cross-stratification, trough cross-

626 stratification, ripple marks). Bedding surfaces separating major sand-bodies include primary

627 substrates that host desiccation cracks, adhesion marks and putative microbial sedimentary

628 surface textures (e.g., *Manchuriophycus,* reticulate marks), which developed during prolonged

629 intervals of sedimentary stasis. The vertical stacking of sedimentary structures in accordance

630 with decreasing associated flow velocity, as well as evidence of periodic emergence and non-

631 deposition, suggests event sedimentation during episodic floods. This degree of interpretation

632 was only achievable due to specific sedimentary conditions at the time of deposition; namely

633 the combination of (1) rapidly decelerating flows acting under aggrading bed conditions; and

634 (2) intervals of non-deposition, during which primary sedimentary surface textures were

635 imparted onto the substrate. Confidence in the interpretation of these depositional processes

636 was attainable despite the fact that the outcrop quality of the Meall Dearg Formation renders it

637 unsuitable for detailed architectural analysis.   In order to promote further robust

638 interpretations from pre-vegetation alluvium of limited outcrop extent, we suggest that the

639 term "sheet-braided" (in inverted commas) continues to be applied or rejected, in order to

640 ensure that the nature of pre-vegetation alluvium may be assessed from worldwide outcrops of

641 varying quality, without recourse to over-interpretation. The depositional characteristics of the

642 Meall Dearg Formation are in line with classical facies models for pre-vegetation alluvium, but

643 we emphasise that our observations do not reveal universal characteristics of Precambrian

644 rivers: they reflect one of a multitude of depositional conditions that could lead to the

645 deposition of "sheet-braided", pre-vegetation alluvium.

646

Acknowledgments and Funding

667 **References**

668 Alexander, J., Bridge, J. S., Cheel, R. J., & Leclair, S. F. (2001) Bedforms and associated

669 sedimentary structures formed under supercritical water flows over aggrading sand beds.

670 *Sedimentology*, 48, 133-152.

671 Alexander, J., & Fielding, C. (1997). Gravel antidunes in the tropical Burdekin River, Queensland,

672 Australia. *Sedimentology*, *44*(2), 327-337.

673 Amor, K., Hesselbo, S. P., Porcelli, D., Thackrey, S., & Parnell, J. (2008) A Precambrian proximal

674 ejecta blanket from Scotland. *Geology*, 36, 303-306.

675 Battison, L., & Brasier, M. D. (2012) Remarkably preserved prokaryote and eukaryote

676 microfossils within 1Ga-old lake phosphates of the Torridon Group, NW Scotland. *Precambrian*

677 *Research*, 196, 204-217.

678 Best, J.L., Ashworth, P.J., Bristow, C.S., Roden, J., 2003. Three-dimensional sedimentary

679 architecture of a large, mid-channel sand braid bar, Jamuna River, Bangladesh. Journal of

680 Sedimentary Research 73, 516-530.

681 Blundell, D. J., Hurich, C. A., & Smithson, S. B. (1985) A model for the MOIST seismic reflection

682 profile, N Scotland. *Journal of the Geological Society*, 142, 245-258.

683 Bradley, W. H. (1933). Factors that determine the curvature of mud-cracked layers. *American*

684 *Journal of Science*, (151), 55-71.

685 Brasier, A. T., Culwick, T., Battison, L., Callow, R. H. T., & Brasier, M. D. (2016) Evaluating

686 evidence from the Torridonian Supergroup (Scotland, UK) for eukaryotic life on land in the

687 Proterozoic. *Geological Society, London, Special Publications*, 448.

688 Bristow, C.S., 1987. Brahmaputra River: channel migration and deposition.

689 Callow, R. H., Battison, L., & Brasier, M. D. (2011) Diverse microbially induced sedimentary

690 structures from 1Ga lakes of the Diabaig Formation, Torridon Group, northwest Scotland.

691 *Sedimentary Geology*, 239, 117-128.

692   British Geological Survey Lexicon of Named Rock Units [online resource]

693   http://www.bgs.ac.uk/lexicon/lexicon.cfm?pub=TAD. Accessed 5th May 2017.

694   Cartigny, M. J., Ventra, D., Postma, G., & Den Berg, J. H. (2014) Morphodynamics and sedimentary

695   structures of bedforms under supercritical-flow conditions: New insights from flume

696   experiments. *Sedimentology*, 61, 712-748.

697   Chavdarian, G. V., & Sumner, D. Y. (2011). Origin and evolution of polygonal cracks in hydrous

698   sulphate sands, White Sands National Monument, New Mexico. *Sedimentology*, *58*(2), 407-423.

699   Corenblit, D., Davies, N. S., Steiger, J., Gibling, M. R., & Bornette, G. (2015). Considering

700   river structure and stability in the light of evolution: feedbacks between riparian

701   vegetation and hydrogeomorphology. *Earth Surface Processes and Landforms*, *40*(2),

702   189-207.

703   Cotter, E., 1978. The evolution of fluvial style, with special reference to the central Appalachian

704   Paleozoic. In: Miall, A.D. (Ed.), Fluvial Sedimentology: Canadian Society of Petroleum Geologists

705   Memoir, vol. 5, 361–383.

706   Dalrymple, R. W., Narbonne, G. M., & Smith, L. (1985). Eolian action and the distribution of

707   Cambrian shales in North America. *Geology*, *13*(9), 607-610.

708   Davies, N. S., & Gibling, M. R. (2010) Cambrian to Devonian evolution of alluvial systems: the

709   sedimentological impact of the earliest land plants. *Earth-Science Reviews*, 98, 171-200.

710   Davies, N. S., Gibling, M. R., & Rygel, M. C. (2011). Alluvial facies evolution during the Palaeozoic

711   greening of the continents: case studies, conceptual models and modern analogues.

712   *Sedimentology*, *58*, 220-258.

713   Davies, N.S., Gibling, M.R., McMahon, W.J., Slater, B.J., Long, D.G.F., Bashforth, A.R., Berry, C.M.,

714   Falcon-Lang, H.J., Gupta, S., Rygel, M.C., & Wellman, C.H. (2017a), Discussion on 'Tectonic and

715   environmental controls on Palaeozoic fluvial environments: reassessing the impacts of early

716   land plants on sedimentation'. Journal of the Geological Society,

717   https://doi.org/10.1144/jgs2016-063. Journal of the Geological Society, first published online

718   [month] [date], [year], https://doi.org/10.1144/JGS2017-004

719   Davies, N. S., Liu, A. G., Gibling, M. R., & Miller, R. F. (2016) Resolving MISS conceptions and

720   misconceptions: A geological approach to sedimentary surface textures generated by microbial

721   and abiotic processes. *Earth-Science Reviews*, 154, 210-246.

722   Davies, N.S., Shillito, A.P., McMahon, W.J. (2017b). Short-term evolution of primary sedimentary

723   surface textures (microbial, ichnological) on a dry stream bed: modern observations and

724   ancient implications. *Palaios*, 32, 125-134.

725   de Almeida, R. P., Marconato, A., Freitas, B. T., & Turra, B. B. (2016). The ancestors of

726   meandering rivers. *Geology*, *44*(3), 203-206.

727   De Boer, P. D. (1981). Mechanical effects of micro-organisms on intertidal bedform migration.

728   *Sedimentology*, *28*(1), 129-132.

729   Endo, R. (1933) Manchuriophycus nov. gen., from a Sinian formation of South Manchuria.

730   *Japanese Jour. Geol. Geogr*, 11, 1-2.

731   Eriksson, P. G. (2007). Classification of structures left by microbial mats in their host sediments.

732   In *Atlas of microbial mat features preserved within the siliciclastic rock record* (p. 39).

733

734   Fedo, C. M., & Cooper, J. D. (1990) Braided fluvial to marine transition: the basal Lower

735   Cambrian Wood Canyon Formation, southern Marble Mountains, Mojave Desert, California.

736   *Journal of Sedimentary Research*, 60.

737   Field, J. (2001). Channel avulsion on alluvial fans in southern Arizona. *Geomorphology*, *37*(1),

738   93-104.

739   Fielding, C. R. (2006) Upper flow regime sheets, lenses and scour fills: extending the range of

740   architectural elements for fluvial sediment bodies. *Sedimentary Geology*, 190, 227-240.

741   Fralick, P. (1999) Paleohydraulics of chute-and-pool structures in a Paleoproterozoic fluvial

742   sandstone. *Sedimentary Geology*, 125, 129-134.

743   Friend, P.F. (1983), Towards the field classification of alluvial architecture or sequence, in

744   Collinson, J.D., and Lewin, J., eds., Modern and Ancient Fluvial Systems: International Association

745   of Sedimentologists, Special Publication 6, p. 345–354.

746   Friend, P.F., Slater, M.J., AND Williams, R.C., 1979, Vertical and lateral building of river sandstone

747   bodies, Ebro Basin, Spain: Geological Society of London, Journal, v. 136, p. 39–46.

748   Fryberger, S. G., Schenk, C. J., & Krystinik, L. F. (1988) Stokes surfaces and the effects of near-

749   surface groundwater-table on Aeolian deposition. *Sedimentology*, 35, 21-41.

750   Fuller, A.O., 1985 A contribution to the conceptual modelling of pre-Devonian fluvial

751   systems. *Transactions Geological Society of South Africa* 88, 189–194.

752   Gibling, M. R., Davies, N. S., Falcon-Lang, H. J., Bashforth, A. R., DiMichele, W. A., Rygel, M. C., &

753   Ielpi, A. (2014) Palaeozoic co-evolution of rivers and vegetation: a synthesis of current

754   knowledge. *Proceedings of the Geologists' Association*, 125, 524-533.

755   Glumac, B., Curran, H. A., Motti, S. A., Weigner, M. M., & Pruss, S. B. (2011) Polygonal sandcracks:

756   Unique sedimentary desiccation structures in Bahamian ooid grainstone. *Geology*, 39, 615-618.

757   Gouramanis, C., Webb, J. A., & Warren, A. A. (2003) Fluviodeltaic sedimentology and ichnology of

758   part of the Silurian Grampians Group, western Victoria. *Australian Journal of Earth Sciences*, 50,

759   811-825.

760   Gracie, A. J., & Stewart, A. D. (1967) Torridonian sediments at Enard Bay, Ross-shire. *Scottish

761   Journal of Geology*, 3, 181-194.

762   Häntzschel,W., (1962) Trace fossils and Problematica. In: Moore, R.C. (Ed.), Treatise on

763   Paleontology (Part W, Conodonts, Conoidal Shells of Uncertain Affinities,Worms, Trace

764   Fossils, Problematica). Geological Society of America, Boulder, Colorado, and University

765   of Kansas, Lawrence. 177–245.

766   Holbrook, J., Scott, R. W., & Oboh-Ikuenobe, F. E. (2006). Base-level buffers and buttresses: a

767   model for upstream versus downstream control on fluvial geometry and architecture within

768   sequences. *Journal of Sedimentary Research*, *76*(1), 162-174.

769   Horton, A.J., Constantine, J.A., Hales, T.C., Goossens, B., Bruford, M.W., & Lazarus, E.D. (2017)

770   Modification of river meandering by tropical deforestation. *Geology*, doi:10.1130/G38740.1

771   Hunter, R. E. (1977) Basic types of stratification in small eolian dunes. *Sedimentology*, 24, 361-

772   387.

773   Hupp, C. R., & Osterkamp, W. R. (1996) Riparian vegetation and fluvial geomorphic processes.

774   *Geomorphology*, 14, 277-295.

775   Ielpi, A., & Ghinassi, M. (2015) Planview style and palaeodrainage of Torridonian channel belts:

776   Applecross Formation, Stoer Peninsula, Scotland. *Sedimentary Geology*, 325, 1-16.

777   Ielpi, A., & Rainbird, R. H. (2015). Architecture and morphodynamics of a 1· 6 Ga fluvial

778   sandstone: Ellice Formation of Elu Basin, Arctic Canada. *Sedimentology*, *62*(7), 1950-1977.

779   Ielpi, A., & Rainbird, R. H. (2016a) Highly Variable Precambrian Fluvial Style Recorded In the

780   Nelson Head Formation of Brock Inlier (Northwest Territories, Canada). *Journal of Sedimentary*

781   *Research*, 86, 199-216.

782   Ielpi, A., & Rainbird, R. H. (2016b) Reappraisal of Precambrian sheet-braided rivers: Evidence

783   for 1· 9 Ga deep-channelled drainage. *Sedimentology*.

784   Ielpi, A., Ventra, D., & Ghinassi, M. (2016) Deeply channelled Precambrian rivers: Remote

785   sensing and outcrop evidence from the 1.2 Ga Stoer Group of NW Scotland. *Precambrian*

786   *Research*.

787   Kennedy, J. F. (1963) The mechanics of dunes and antidunes in erodible-bed channels. *Journal of*

788   *Fluid Mechanics*, 16, 521-544.

789   Kinnaird, T. C., Prave, A. R., Kirkland, C. L., Horstwood, M., Parrish, R., & Batchelor, R. A. (2007)

790   The late Mesoproterozoic–early Neoproterozoic tectonostratigraphic evolution of NW Scotland:

791   the Torridonian revisited. *Journal of the Geological Society*, 164, 541-551.

792   Kocurek, G. (1981) Significance of interdune deposits and bounding surfaces in aeolian dune

793   sands. *Sedimentology*, 28, 753-780.

794   Kocurek, G. (1996) Desert aeolian systems.

795   Kocurek, G., & Fielder, G. (1982) Adhesion structures. *Journal of Sedimentary Research*, 52(4).

796   Kocurek, G., & Havholm, K. G. (1993) Eolian sequence stratigraphy-a conceptual framework.

797   Memoirs-American Association of Petroleum Geologists, 393-393.

798   Kocurek, G., & Nielson, J. (1986). Conditions favourable for the formation of warm-

799   climate aeolian sand sheets. *Sedimentology*, *33*(6), 795-816.

800   Koehn, D., Bons, P., Montenari, M., & Seilacher, A. (2014) The elastic age: rise and fall of

801   Precambrian biomat communities. In *EGU General Assembly Conference Abstracts* (Vol. 16, p.

802   13793).

803   Kovalchuk, O., Owttrim, G. W., Konhauser, K. O., & Gingras, M. K. (2017). Desiccation cracks in

804   siliciclastic deposits: Microbial mat-related compared to abiotic sedimentary origin.

805   *Sedimentary Geology*, *347*, 67-78.

806   Krabbendam, M. (2012) Stoer Group at Enard Bay. In Goodenough, K.M. & Krabbendam, M.

807   (eds.) A Geological Excursion Guide to the North-West Highlands of Scotland. Edinburgh

808   Geological Society, Edinburgh, pp. 74-84.

809   Krynine, P. D. (1948) The megascopic study and field classification of sedimentary rocks:

810   Journal of Geology, v. 56, p. 130–165.

811   Lancaster, N., & Baas, A. (1998) Influence of vegetation cover on sand transport by wind: field

812   studies at Owens Lake, California. *Earth Surface Processes and Landforms*, 23, 69-82.

813   Langford, R. P. (1989). Fluvial-aeolian interactions: Part I, modern systems. *Sedimentology*,

814   *36*(6), 1023-1035.

815 Long, D. G. (2006). Architecture of pre-vegetation sandy-braided perennial and ephemeral river

816 deposits in the Paleoproterozoic Athabasca Group, northern Saskatchewan, Canada as

817 indicators of Precambrian fluvial style. *Sedimentary Geology*, *190*(1), 71-95.

818 Lowe, D. G., & Arnott, R. W. C. (2016) Composition and Architecture of Braided and Sheetflood-

819 Dominated Ephemeral Fluvial Strata In the Cambrian–Ordovician Potsdam Group: A Case

820 Example of the Morphodynamics of Early Phanerozoic Fluvial Systems and Climate Change.

821 *Journal of Sedimentary Research*, 86, 587-612.

822 MacCulloch, J. (1819) A description of the western islands of Scotland, including the Isle of Man,

823 comprising an account of their geological structures, with remarks on their agriculture, scenery

824 and antiques. Constable, London, 3 Vols.

825 Marconato, A., de Almeida, R. P., Turra, B. B., & dos Santos Fragoso-Cesar, A. R. (2014) Pre-

826 vegetation fluvial floodplains and channel-belts in the Late Neoproterozoic–Cambrian Santa

827 Bárbara group (Southern Brazil). *Sedimentary Geology*, 300, 49-61.

828 McKee, E. D., Crosby, E. T., & Berryhill Jr, H. L. (1967). Flood deposits, Bijou Creek, Colorado, June

829 1965. *Journal of Sedimentary Research*, 37.

830 McMahon, S., van Smeerdijk Hood, A., & McIlroy, D. (2016). The origin and occurrence of

831 subaqueous sedimentary cracks. *Geological Society, London, Special Publications*, *448*, SP448-15.

832 McMahon, W. J., Davies, N. S., & Went, D. J. (2017). Negligible microbial matground influence on

833 pre-vegetation river functioning: Evidence from the Ediacaran-Lower Cambrian Series Rouge,

834 France. *Precambrian Research*, *292*, 13-34.

835 McManus, J., & Bajabaa, S. (1998). The importance of air escape processes in the formation of

836 dish-and-pillar and teepee structures within modern and Precambrian fluvial deposits.

837 *Sedimentary geology*, 120, 337-343.

838 Miall, A. D. (1985). Architectural-element analysis: a new method of facies analysis applied to

839 fluvial deposits. *Earth-Science Reviews*, *22*(4), 261-308.

840   Miall, A. D. (2014). *Fluvial depositional systems* (Vol. 14). Berlin: Springer.

841   Minter, N. J., Buatois, L. A., & Mángano, M. G. (2016). The conceptual and methodological tools of

842   ichnology. In *The Trace-Fossil Record of Major Evolutionary Events* (pp. 1-26). Springer

843   Netherlands.

844   Moor, H., Rydin, H., Hylander, K., Nilsson, M. B., Lindborg, R., & Norberg, J. (2017). Towards a

845   trait-based ecology of wetland vegetation. *Journal of Ecology*.

846   Mountney, N. P. (2004). Feature: The sedimentary signature of deserts and their response to

847   environmental change. *Geology Today*, 20, 101-106.

848   Mountney, N. P. (2012). A stratigraphic model to account for complexity in aeolian dune and

849   interdune successions. *Sedimentology*, 59, 964-989.

850   Nicholson, P.G., (1993) A basin reappraisal of the Proterozoic Torridon Group, northwest

851   Scotland. In: Frostick, L., Steel, R.J. (Eds.), Tectonic Controls and Signatures in

852   Sedimentary Successions. *Special Publications of the International Association of*

853   *Sedimentologists*, 20, 183–202.

854   Noffke, N., Gerdes, G., Klenke, T., & Krumbein, W. E. (2001) Microbially Induced Sedimentary

855   Structures--A New Category within the Classification of Primary Sedimentary Structures:

856   Perspectives. *Journal of Sedimentary Research*, 71, 649-656.

857   North, C. P., & Davidson, S. K. (2012). Unconfined alluvial flow processes: recognition and

858   interpretation of their deposits, and the significance for palaeogeographic reconstruction.

859   *Earth-Science Reviews*, *111*, 199-223.

860   Owen, G. (1995) Soft-sediment deformation in upper Proterozoic Torridonian sandstones

861   (Applecross Formation) at Torridon, northwest Scotland. *Journal of Sedimentary Research*, 65.

862   Owen, G., Santos, M.G.M., (2014) Soft-sediment deformation in a pre-vegetation river system:

863   the Neoproterozoic Torridonian of NW Scotland. *Proceedings of the Geologists' Association*, 125,

864   511–523.

865   Paola, C. H. R. I. S., Wiele, S. M., & Reinhart, M. A. (1989) Upper-regime parallel lamination as the

866   result of turbulent sediment transport and low-amplitude bed forms. *Sedimentology*, 36, 47-59.

867   Park, R. G., Stewart, A. D., & Wright, D. T. (2002). The Hebridean terrane. *The Geology of Scotland.*

868   *Geological Society, London*, 45-80.

869   Parnell, J., Mark, D., Fallick, A.E., Boyce, A., Thackrey, S., (2011) The age of the Mesoproterozoic

870   Stoer Group sedimentary and impact deposits, NWScotland. *Journal of the Geological Society,*

871   *London*, 168, 349–358.

872   Peach, B.N., Horne, J., Gunn,W., Clough, C.T., Hinxman, L.W., Teall, J.J.H., (1907) The geological

873   structure of the northwest highlands of Scotland. *Memoirs of the Geological Survey of Scotland.*

874   Prave, A. R. (2002) Life on land in the Proterozoic: Evidence from the Torridonian rocks of

875   northwest Scotland. *Geology*, 30, 811-814.

876   Rainbird, R. H. (1992). Anatomy of a large-scale braid-plain quartzarenite from the

877   Neoproterozoic Shaler Group, Victoria Island, Northwest Territories, Canada. *Canadian Journal*

878   *of Earth Sciences*, *29*(12), 2537-2550.

879   Rainbird, R., Cawood, P., & Gehrels, G. (2012) The great Grenvillian sedimentation episode:

880   Record of supercontinent Rodinia's assembly. *Tectonics of Sedimentary Basins: Recent Advances:*

881   *Blackwell Publishing Ltd*, 583-601.

882   Reid, I. & Frostick, L.E. (1994) Fluvial sediment transport and deposition. In *Sediment Transport*

883   *and Depositional Processes* (ed Pye K). Blackwell Scientific Publications, Oxford, pp. 89-156.

884   Reesink, A. J. H., Van den Berg, J. H., Parsons, D. R., Amsler, M. L., Best, J. L., Hardy, R. J., Orfea. O &

885   Szupiany, R. N. (2015) Extremes in dune preservation: Controls on the completeness of fluvial

886   deposits. *Earth-Science Reviews*, 150, 652-665.

887   Santos, M. G., Almeida, R. P., Godinho, L. P., Marconato, A., & Mountney, N. P. (2014) Distinct

888   styles of fluvial deposition in a Cambrian rift basin. *Sedimentology*, 61, 881-914.

889

890   Santos, M. G., & Owen, G. (2016) Heterolithic meandering-channel deposits from the

891   Neoproterozoic of NW Scotland: Implications for palaeogeographic reconstructions of

892   Precambrian sedimentary environments. *Precambrian Research*, 272, 226-243.

893   Saunderson, H. C., & Lockett, F. P. (1983) Flume experiments on bedforms and structures at the

894   dune-plane bed transition. In *Modern and Ancient Fluvial Systems* (Vol. 6, pp. 49-58).

895   International Association of Sedimentologists.

896   Schumm, S.A. (1968) Speculations concerning paleohydraulic controls of terrestrial

897   sedimentation. Geological Society of America Bulletin, 79, 1573–1588.

898   Schieber, J. (1999) Microbial mats in terrigenous clastics: the challenge of identification in the

899   rock record. Palaios, 14, 3–13.

900   Schieber J. (2007) Ripple patches in the Cretaceous Dakota Sandstone near Denver, Colorado, a

901   classic locality for microbially bound tidal sand flats. In Atlas of Microbial Mat Features

902   Preserved Within the Siliciclastic Rock Record (eds Schieber J, Bose PK, Eriksson PG, Banerjee S,

903   Sarkar S, Altermann W, Catuneanu O). Atlases in Geosciences. Elsevier, Amsterdam, pp. 222–

904   225.

905   Sedgwick, A., Muchison R.I. (1835). On the structure and the relations of the deposits

906   constrained between the Primary rocks and the Oolitic Series in the north of Scotland.

907   *Transactions of the Geological Society of London,* 2nd series, 3, 125 - 160

908   Selley, R. C. (1965) Diagnostic characters of fluviatile sediments of the Torridonian formation

909   (Precambrian) of northwest Scotland. *Journal of Sedimentary Research*, 35.

910   Shepard, R.N., Sumner, D.Y., (2010) Undirected motility of filamentous cyanobacteria produces

911   reticulate mats. *Geobiology*, 8, 179–190.

912   Simms, M. J. (2015) The Stac Fada impact ejecta deposit and the Lairg Gravity Low: evidence for

913   a buried Precambrian impact crater in Scotland?. *Proceedings of the Geologists' Association*, 126,

914   742-761.

915   Smith, R. L., Stearn, J. E. F., & Piper, J. D. A. (1983) Palaeomagnetic studies of the Torridonian

916   sediments, NW Scotland. *Scottish Journal of Geology*, 19(1), 29-45.

917   Stein, A. M. (1988) Basement controls upon basin development in the Caledonian foreland, NW

918   Scotland. *Basin Research*, 1, 107-119.

919   Stein, A. M. (1992) Basin development and petroleum potential in The Minches and Sea of the

920   Hebrides Basins. *Geological Society, London, Special Publications*, 62, 17-20.

921   Stewart, A.D., (1969). Torridonian rocks of Scotland reviewed. In: Kay, M. (Ed.), North

922   Atlantic—Geology and Continental Drift: A Symposium. *American Association of Petroleum*

923   *Geologists Memoir*, 12, 595–608.

924   Stewart, A.D., (1982). Late Proterozoic rifting in NW Scotland: the genesis of the

925   'Torridonian'. Journal of the Geological Society, London, 139, 413–420.

926   Stewart, A. D. (1990). Geochemistry, provenance and climate of the Upper Proterozoic Stoer
927   Group in Scotland. *Scottish Journal of Geology*, *26*(2), 89-97.
928

929   Stewart, A. D. (1991). Geochemistry, provenance and palaeoclimate of the Sleat and Torridon

930   groups in Skye. *Scottish Journal of Geology*, 27, 81-95.

931   Stewart, A.D., (2002). The later Proterozoic Torridonian rocks of Scotland: their sedimentology,

932   geochemistry, and origin. *Geological Society, London, Memoir*, 24.

933   Stewart, A.D., Donnellan, N.C.B., (1992). Geochemistry and provenance of red sandstones in the

934   Upper Proterozoic Torridon Group in Scotland. Scottish Journal of Geology 28,143–153.

935   Stewart and Irving, E (1974) Palaeomagnetism of Precambrian sedimentary rocks from north-

936   west Scotland and the apparent polar wander path of Laurentia. *Geophys. f. R. Astron. Soc.* 37, 57-

937   72.

938   Strother, P. K., & Wellman, C. H. (2016) Palaeoecology of a billion-year-old non-marine

939   cyanobacterium from the Torridon Group and Nonesuch Formation. *Palaeontology*, *59*(1), 89-

940   108.

941   Strother, P. K., Battison, L., Brasier, M. D., & Wellman, C. H. (2011) Earth/'s earliest non-marine

942   eukaryotes. *Nature*, 473, 505-509.

943   Teall, J.J.H. (1907) The Petrography of the Torridonian Formation. *Memoirs of the*

944   *Geological Survey of Great Britain*, 278–290.

945   Thorne, C.R. (1990) Effects of vegetation on Riverbank erosion and stability. In: Thornes,

946   J.W. (Ed.), Vegetation and Erosion: Processes and Environments. John Wiley and Sons,

947   Chichester, 125–144.

948   Tipper, J. C. (2015). The importance of doing nothing: stasis in sedimentation systems and its

949   stratigraphic effects. *Geological Society, London, Special Publications*, *404*(1), 105-122.

950   Tirsgaard, H., & Øxnevad, I. E. (1998) Preservation of pre-vegetational mixed fluvio–aeolian

951   deposits in a humid climatic setting: an example from the Middle Proterozoic Eriksfjord

952   Formation, Southwest Greenland. *Sedimentary Geology*, 120, 295-317.

953   Todd, S. P., & Went, D. J. (1991). Lateral migration of sand-bed rivers: examples from the

954   Devonian Glashabeg Formation, SW Ireland and the Cambrian Alderney Sandstone Formation,

955   Channel Islands. *Sedimentology*, *38*(6), 997-1020.

956   Torsvik, T. H., & Sturt, B. A. (1987). On the origin and stability of remanence and the magnetic

957   fabric of the Torridonian Red Beds, NW Scotland. *Scottish Journal of Geology*, *23*(1), 23-38.

958   Trewin, N. H. (1993) Controls on fluvial deposition in mixed fluvial and aeolian facies within the

959   Tumblagooda Sandstone (Late Silurian) of Western Australia. *Sedimentary Geology*, 85, 387-400.

960   Turnbull, M. J., Whitehouse, M. J., & Moorbath, S. (1996) New isotopic age determinations for the

961   Torridonian, NW Scotland. *Journal of the Geological Society*, 153, 955-964.

962   Van de Kamp, P. C., & Leake, B. E. (1997) Mineralogy, geochemistry, provenance and sodium

963   metasomatism of Torridonian rift basin clastic rocks, NW Scotland. *Scottish Journal of Geology*,

964   33, 105-124.

965   Van Mechelen, J. L. M. (2004). Strength of moist sand controlled by surface tension for tectonic

966   analogue modelling. *Tectonophysics*, *384*(1), 275-284.

967   Williams, G. E. (1966) The Precambrian Torridonian sediments of the Cape Wrath district,

968   north-west Scotland. *Univ. Reading Ph.D thesis,* (unpubl.).

969   Williams, G. E. (2001) Neoproterozoic (Torridonian) alluvial fan succession, northwest Scotland,

970   and its tectonic setting and provenance. *Geological Magazine*, 138, 161-184.

971   Williams, G. E., & Foden, J. (2011) A unifying model for the Torridon Group (early

972   Neoproterozoic), NW Scotland: Product of post-Grenvillian extensional collapse. *Earth-Science*

973   *Reviews*, 108, 34-49.

974   Williams, G. E., & Schmidt, P. W. (1997) Palaeomagnetic dating of sub-Torridon Group

975   weathering profiles, NW Scotland: verification of Neoproterozoic palaeosols. *Journal of the*

976   *Geological Society*, 154, 987-997.

977   Winston, D. (2016) Sheetflood sedimentology of the Mesoproterozoic Revett Formation, Belt

978   Supergroup, northwestern Montana, USA. *Geological Society of America Special Papers*, 522

979   Young, G. M. (1999). Some aspects of the geochemistry, provenance and palaeoclimatology of

980   the Torridonian of NW Scotland. *Journal of the Geological Society*, 156, 1097-1111.

981
982

983

984

985

986

987

988

989

990

991

992

993

994   Figure 1. (A) Geological map of the informal Torridonian Supergroup; (B) Higher resolution maps of MDF

995   locations of study; (C) Stratigraphic column of the stratigraphy of the NW Scottish Highlands.

996   Figure 2. Representative stratigraphic logs of Facies Associations 1 and 2. Sr = ripple marks.

997   Figure 3. (A) Planform surfaces at Rubha Réidh. The microtopography of the surface is dictated by the

998   underlying lithofacies. If horizontal-laminations (Sh) comprise the topmost lithofacies of the underlying

999   sand-body, topography is flat (B). If dune cross-stratification comprise the topmost lithofacies of the

1000   underlying sand-body, dune microtopography is preserved (C). Each planform surface is near

1001   ubiquitously covered in ripple marks.

1002   Figure 4. Possible chute and pool structures at: (A) Rubha Réidh; (B) Stoer (inaccessible cliff exposure).

1003   Upstream-dipping bedding truncates against the steeper, down-flow dipping surfaces ('Pool'). Convex up

1004   bedding passes over topographic high ('Chute').

1005   Figure 5. (A) Solitary antidune stratification, with backset cross-bedding dipping against prevailing

1006   palaeoflow; (B) Convex-up bedding possibly representative of antidune stratification. (Both images from

1007   Rubha Réidh)

1008   Figure 6. Architectural panel of Meall Dearg outcrop (Rubha Réidh).

1009   Figure 7. (A) Humpback cross-stratification at Rubha Réidh; (B) Three-dimensional exposures show the

1010   westward outbuilding of wedge-shaped humpback cross-stratified packages. Sh = horizontal-laminations;

1011   Sl = Low-angle cross-stratification; Sr = Ripple marks

1012   Figure 8. (A) Low-angle cross-stratification at Balchladich Bay (Sl); (B) Alternating sets of horizontal-

1013   laminated (Sh) and planar cross-stratified (Sp) sandstones at Stoer.

1014   Figure 9. (A) Ripple marks superimposed onto dune topography; (B) Planar surface with ripple marks

1015   Figure 10. Morphology of preserved ripple-marks: (A) Drainage marks etched in flanks of ripple marks;

1016   (B) Sharp crested ripple crests; (C) Synaeresis cracks in ripple troughs; (D) Interference ripple marks; (E)

1017   Mud draped ripple marks within dune trough; (F) Ripple marks preserved in vertical section; (G)

1018   Oversteepened ripple marks; (H) Desiccated mudstones; (i) Desiccated polygons overprinting rippled

1019   sandstone, no mud preserved. All photos from Rubha Réidh.

1020   Figure 11. Schematic illustration and photographs of adhesion mark distribution across Meall Dearg

1021   fluvial facies.

1022   Figure 12. Examples of *Manchuriophycus* at Rubha Réidh. Fragments of possible '*Manchuriophycus'*

1023   highlighted in red.

1024   Figure 13. Possible microbial sedimentary surface textures at Rubha Réidh: (A, B) Reticulate markings

1025   preserved at Rubha Réidh; (C) Clear margin separating sandstone with and without adhesion marks.

1026   Figure 14. (A) Desiccated sandstone surface; (B) Desiccated mudstone surface. Both Rubha Réidh

1027   Figure 15. (A) Intercalated planar cross-stratified dunes and planar-bedded interdunes at Enard Bay.

1028   Person is 187 cm. Restored to horizontal; (B) Aeolian dune geometry in depositional-dip sections; (C)

1029   Aeolian dune geometry in depositional-strike sections; (D) Large scale arcuate aeolian dune-forms; (E)

1030   Palaeoflow dispersal across an individual aeolian dune-form. All Enard Bay.

1031   Figure 16. Exposure of occasionally pebbly, coarse-grained, cross-bedded sandstone apparently faulted

1032   into contact with the rest of the Meall Dearg Formation at Enard Bay

1033   Figure 17. Sedimentary structures at Enard Bay: (A) Cross laminae in dune facies (interpreted grainflow

1034   deposits). Restored to horizontal; (B) Textural and mineralogical character of dune facies as observed in

1035   thin-sectioned samples under polarized light (C) Planar laminations in dune facies (interpreted grainfall

1036   deposits); (D) Wind-ripple horizontal laminae define pin-stripe laminations; (E) Adhesion warts

1037   preserved on interdune surface; (F) Possible adhesion lamination in interdune facies. Photographs A – D

1038   are not restored to horizontal.

1039   Figure 18. (A) Dune sets separated by low-angle, erosional reactivation surfaces (dashed line). Person is

1040   187 cm; (B) Channel-body incising into 2.4 m thick planar-bedded package (Enard Bay).

1041   Figure 19. Limitations of Meall Dearg Formation coastal exposures for determining large-scale

1042   depositional architecture: (A) Tectonic dip (25-30°) renders the exposure unsuitable for interpretation

1043   from satellite imagery because surficial cross-sectional exposure of beds is oblique to land surface; (B)

1044   Coastal exposure disappears beneath a variably deep drift cover of post-glacial till and peat bog, making it

1045 impossible to trace bedding for greater than 140 m. Photograph restored to horizontal. Meall Dearg

1046 outcrop highlighted in green in both photographs.

1047
1048

1049

1050

1051

1052

1053

1054

1055

1056

1057

1058

1059

1060

1061

1062

1063

1064

1065

1066

1067

1068

1069

1070

1071

1072

1073

1074

1075

1076

1077

1078

1079

1080

1081

1082

1083

1084

1085

1086

1087

1088
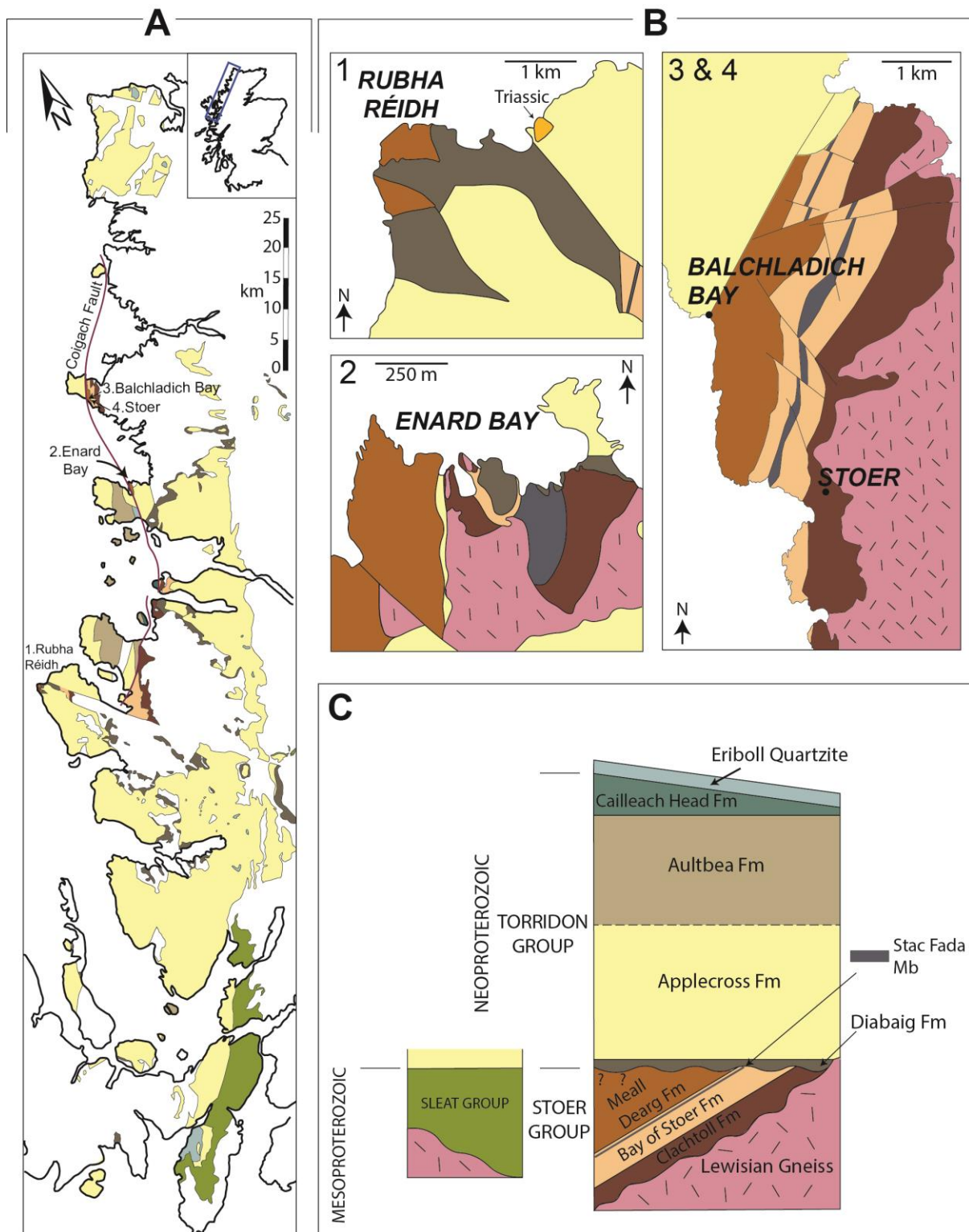
1089

1090

1091

1092

1093

1094

1095

1096

1097

1098

1099

1100

1101

Fig. 1

1102

1103

1104

1105

1106

1107 **Fig. 2**
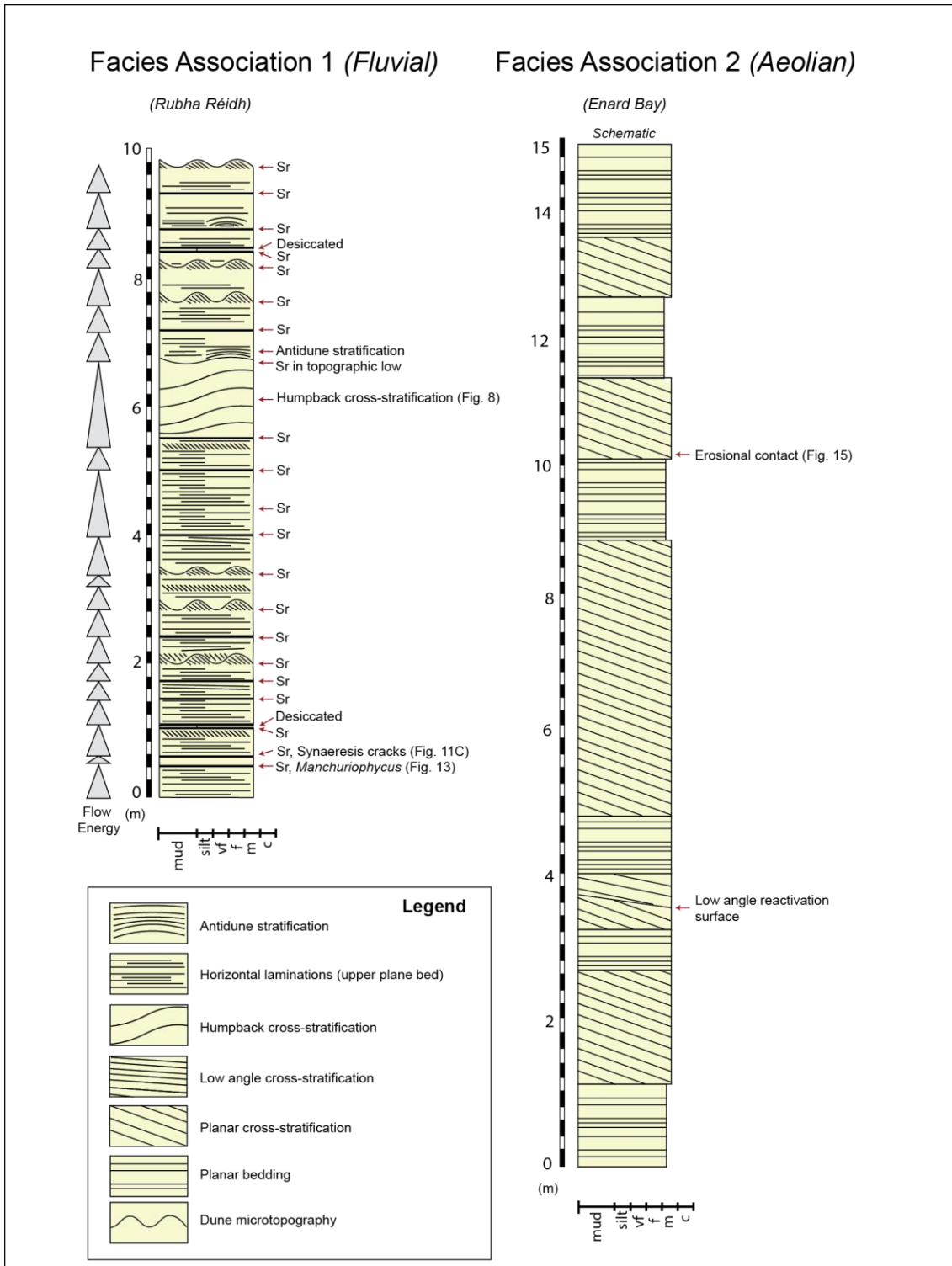
1108

1109

1110

1111

1112

1113

1114   **Fig. 3**

1115

1116   **Fig. 4**

1. Upstream migrating backsets   2. Scour hollow ('**pool**')   3. Convex-up bedding draping over topographic high ('**chute**')

4. Soft-sediment deformation   5. Upstream-dipping scour surface
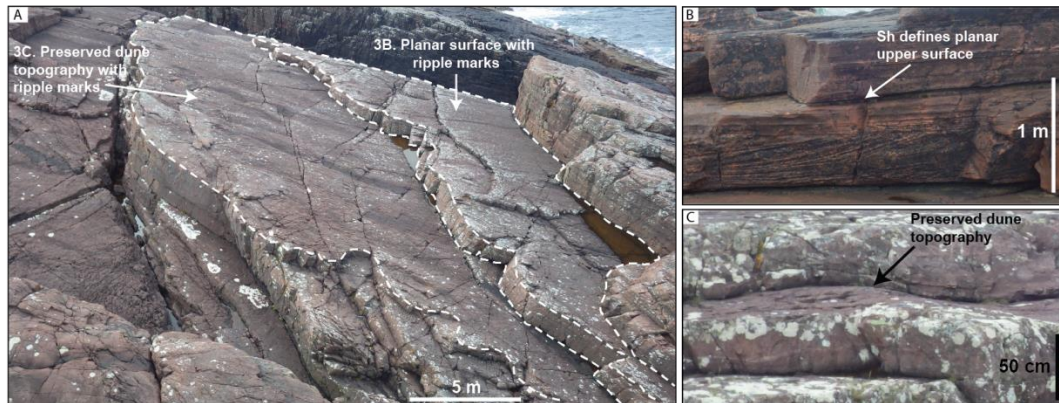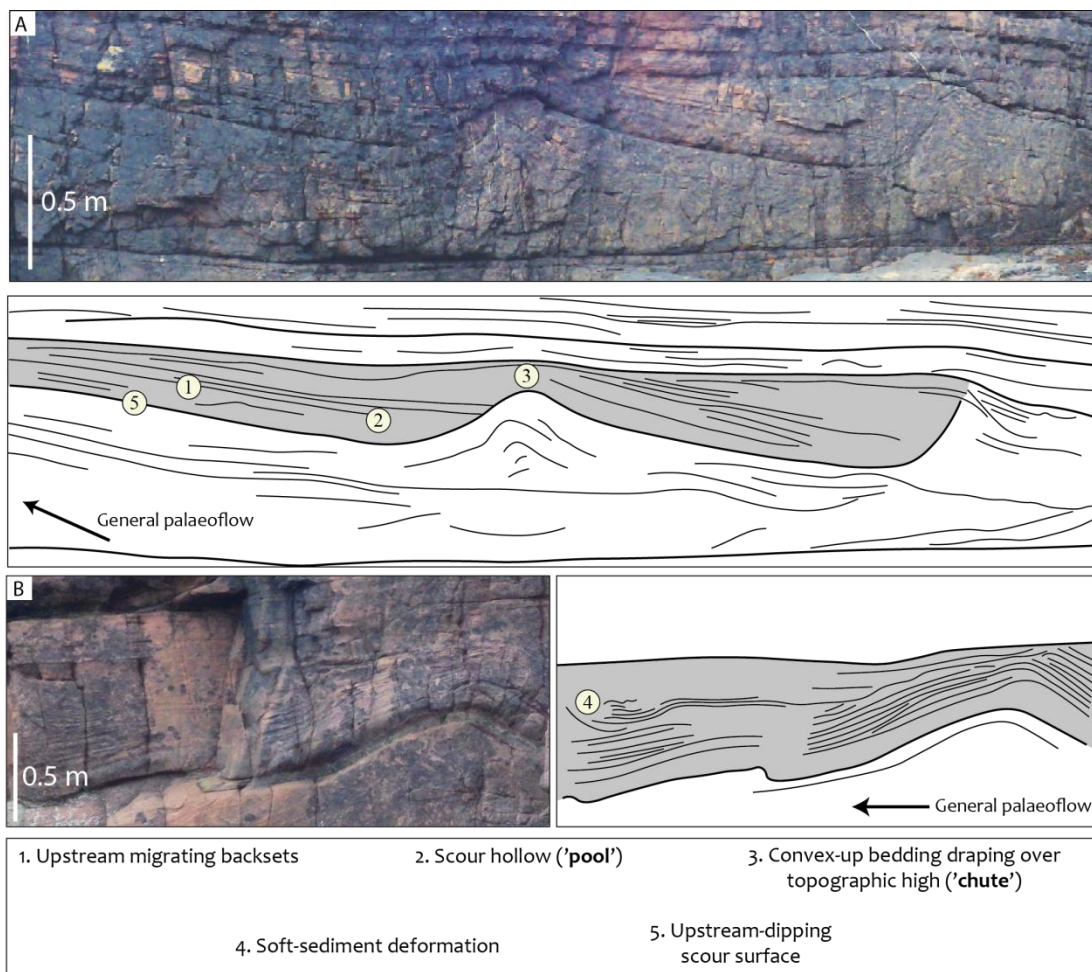
1117

1118

1119

Fig. 5
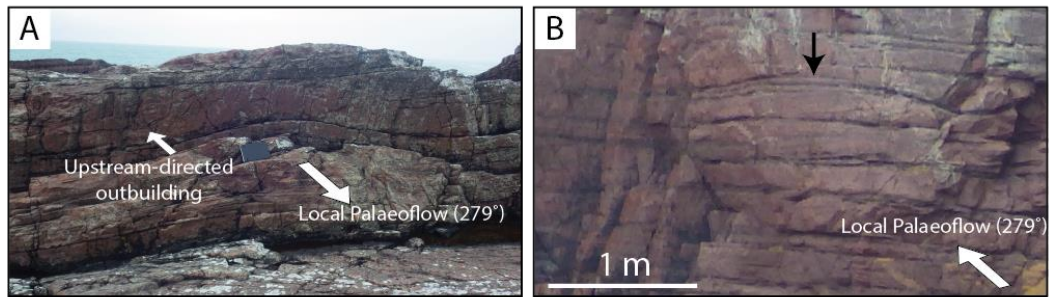
1121

1122
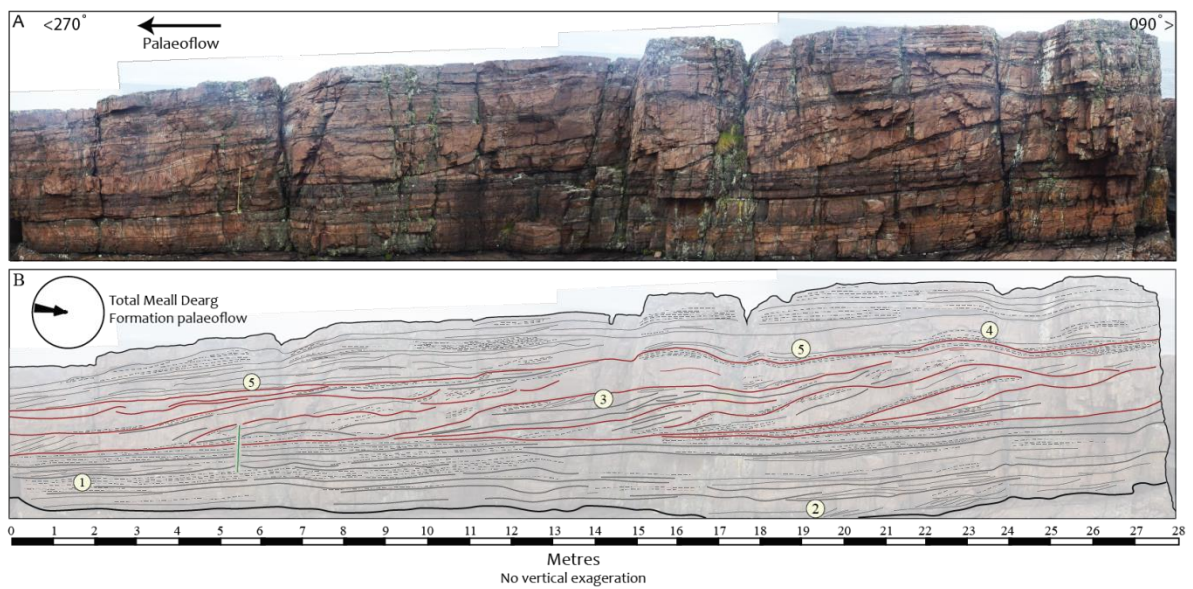
Fig. 6

1124

1125

1126

1127

1128

1129

1130

1131

1132

1133

Fig. 6 (cont)

| Principle bounding surface | Subordinate bounding surface | ----- Well-pronounced stratification | Humpback cross-stratification | Ripple marks |
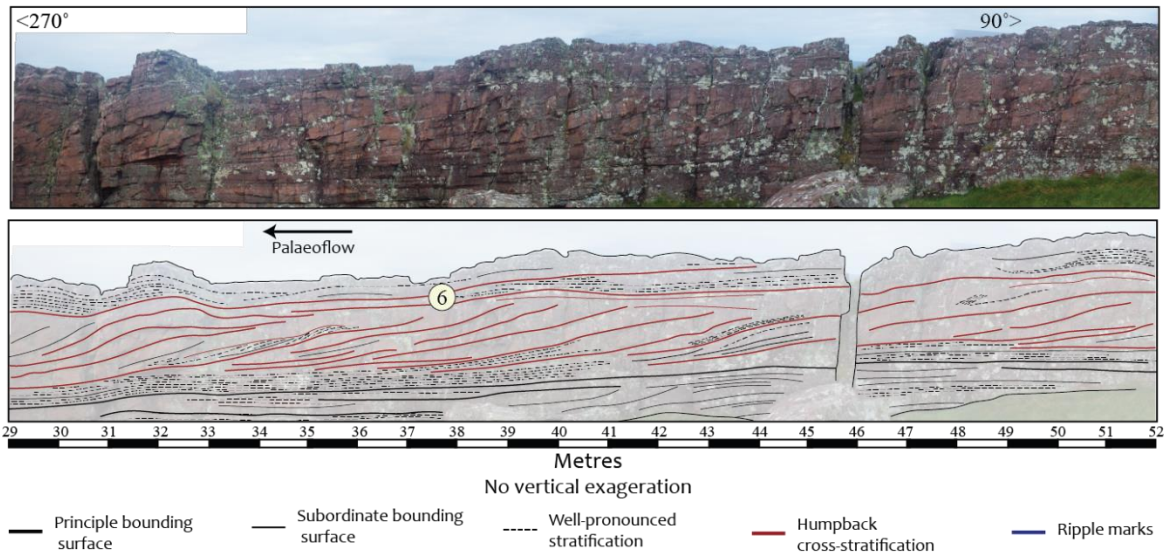
1135

Fig. 6cont
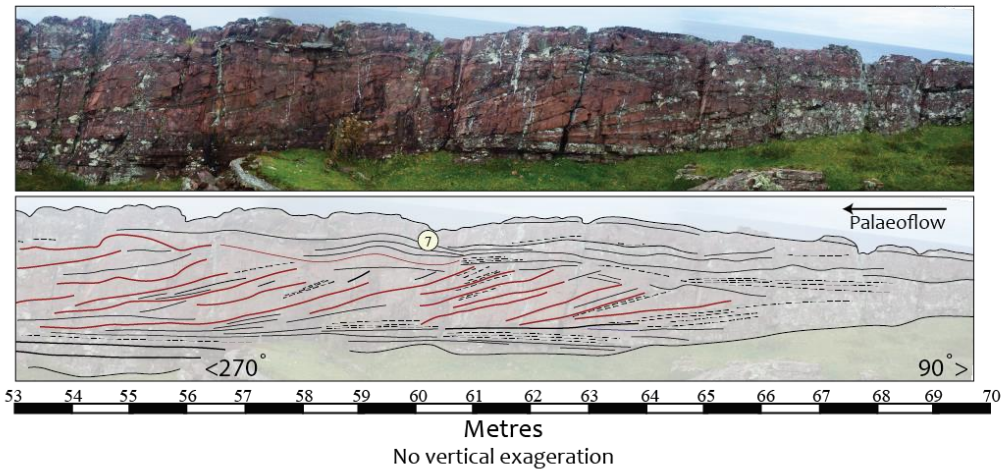
1. Sets of horizontal laminations orgnised within a tabular package. Bottom sets of internal packages dip gently down-flow

2. Lower flow regime cross-stratification are restricted to isolated sets and frequently have top surfaces eroded by horizontal laminations

3. Fig. 7: Humpback cross-stratification. Convex-up bed topography constitutes a form set which grades down-flow (west) into a relatively large foreset and in turn into an extensive, flat-laminated bottomset

4. Low relief, convex-upward, largely symmetrical bedding with backset cross-stratification are interpreted as antidune stratification

5. Above humpback cross-stratification, ripple marks are preserved in troughs only, where water would have pooled during waning flow conditions

6. Horizontal laminated package thins downstream and transitions into humpback cross-stratification

7. Convex-up, symmetrical antidune with backset cross-bedding evolving from underlying humpback cross-stratified package

1137

1138

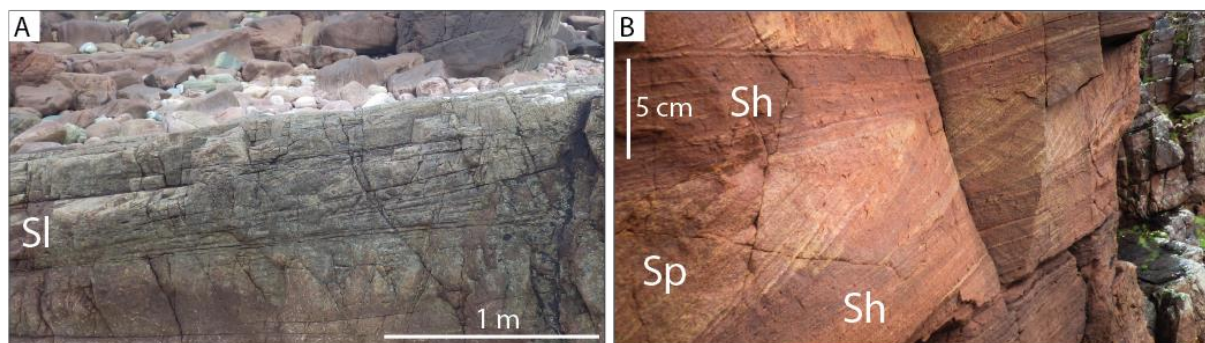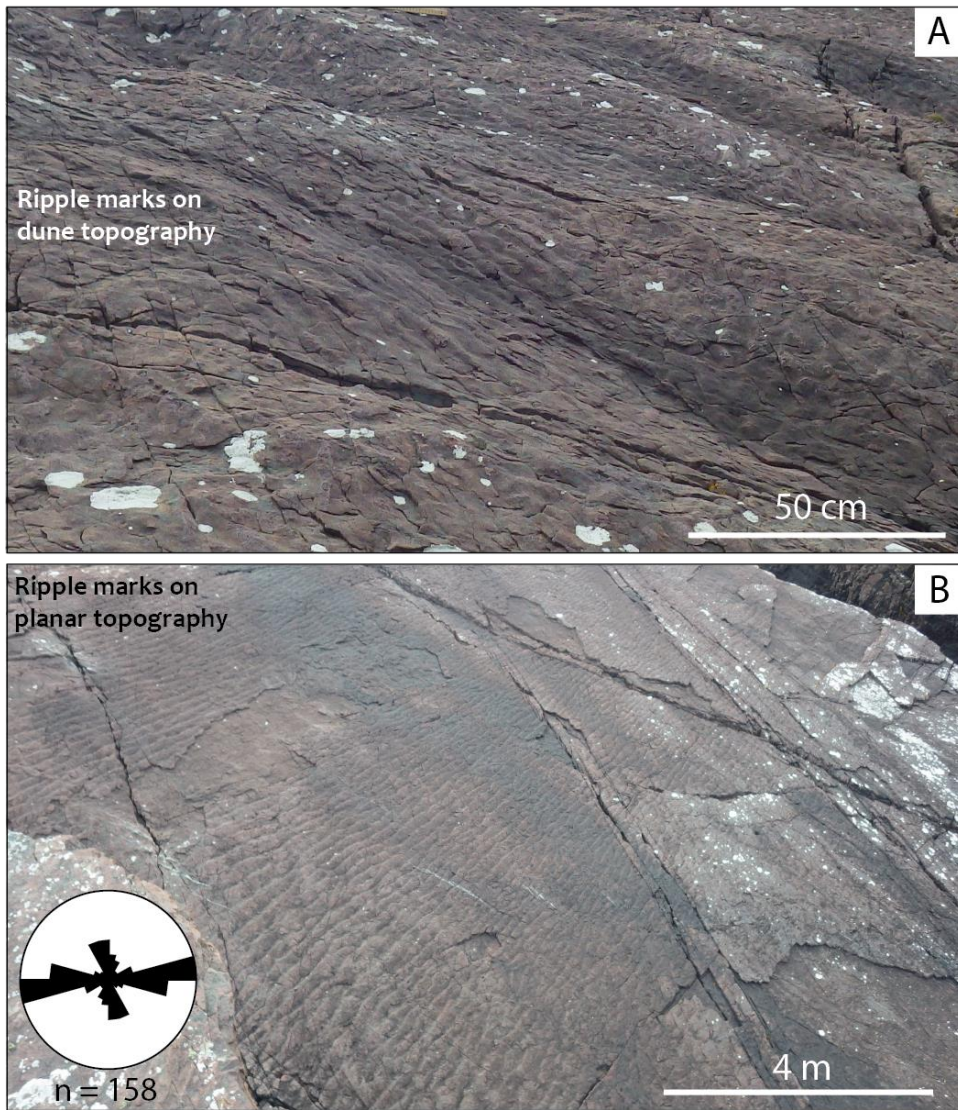1139

1140

1141 **Fig. 7**
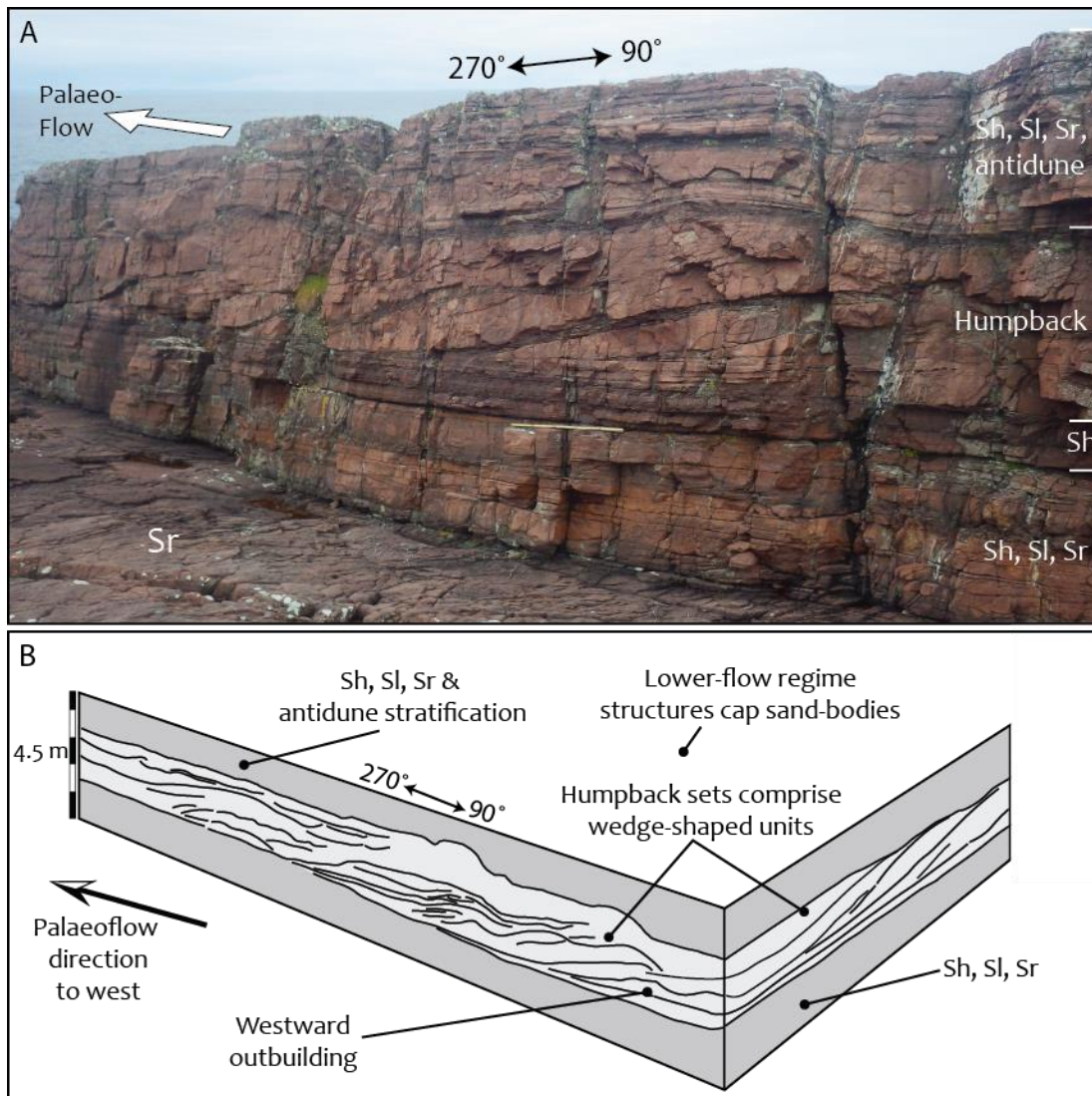
1142

1143

1144 **Fig. 8**

1145

1146

1147

1148

1149   **Fig. 9**

1150

1151

1152

1153

1154

1155
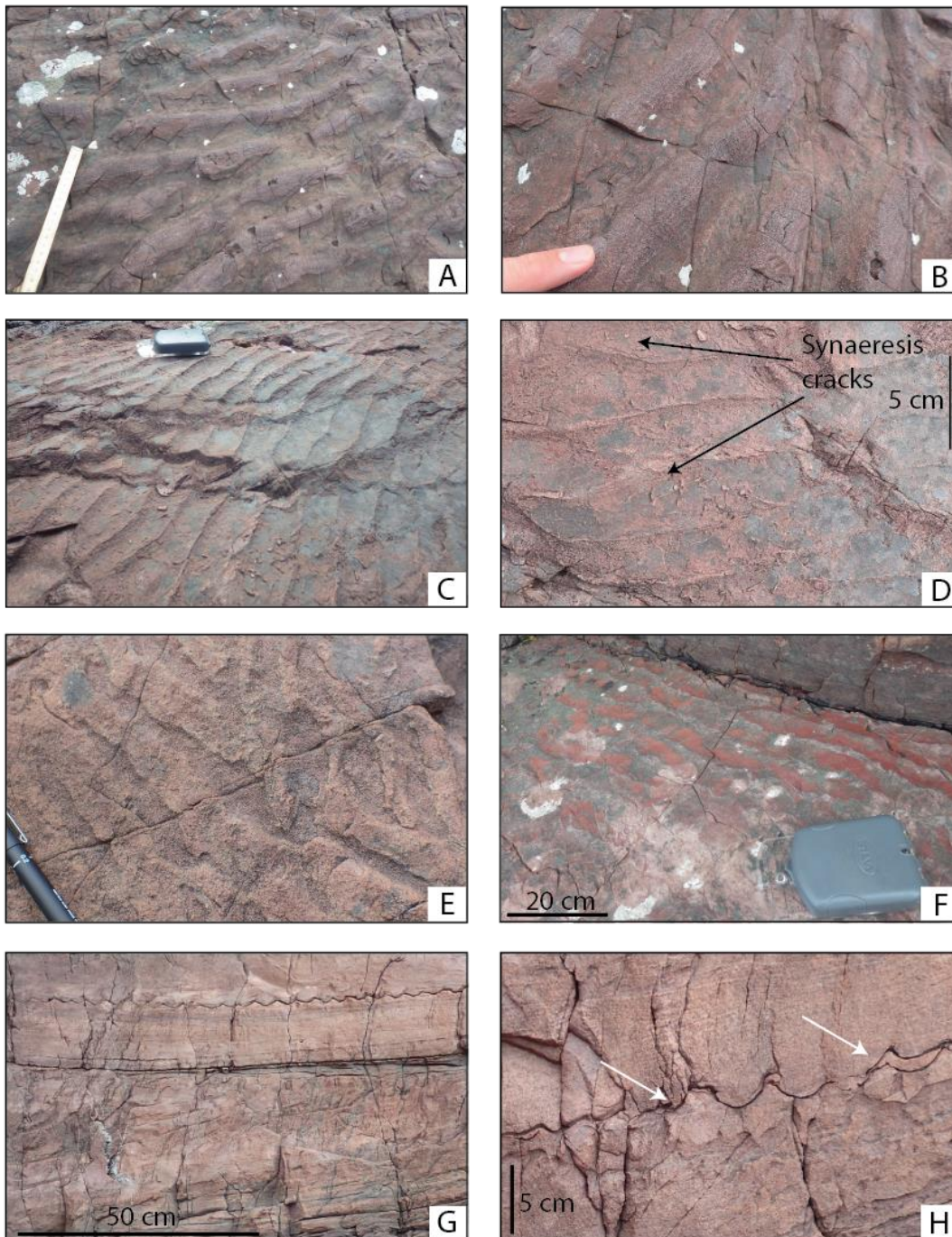
1156

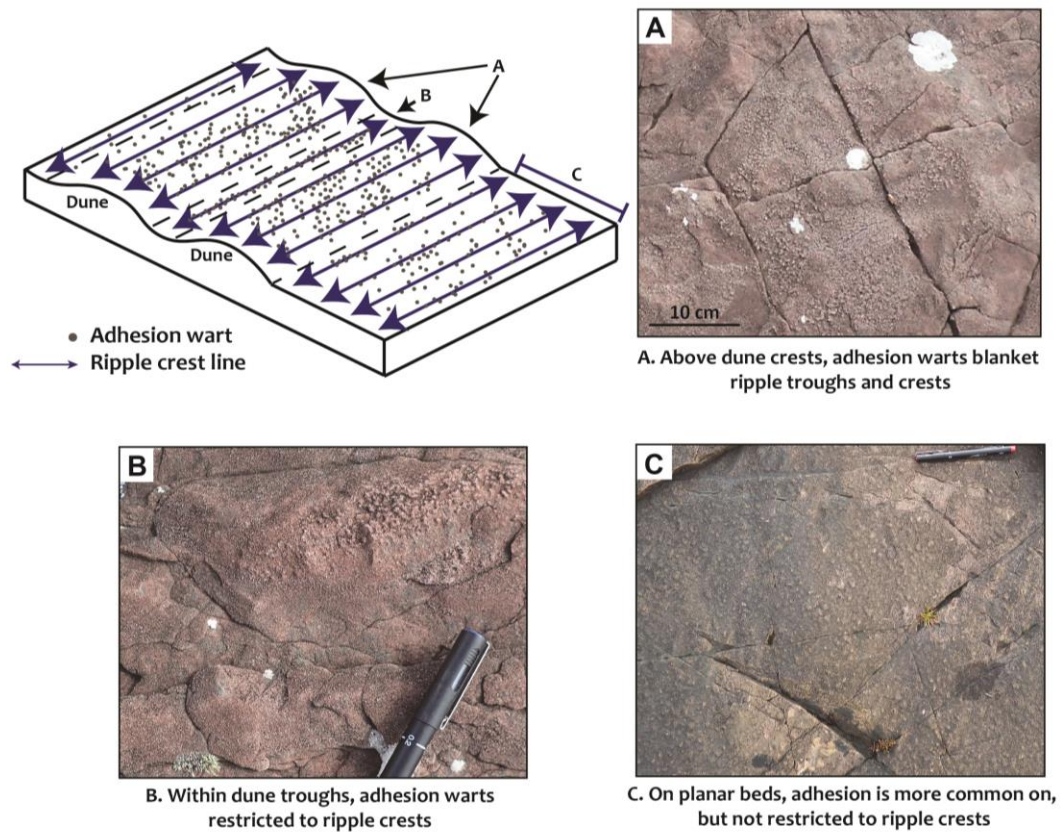1157

1158   **Fig. 10**

1159

1160

1161

1162

1163

1164

1165

1166 **Fig. 11**

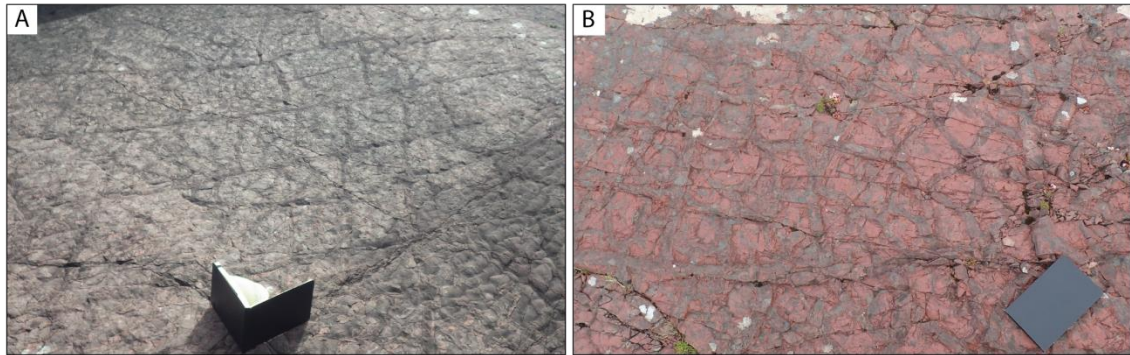A. Above dune crests, adhesion warts blanket
ripple troughs and crests

B. Within dune troughs, adhesion warts
restricted to ripple crests

C. On planar beds, adhesion is more common on,
but not restricted to ripple crests

- Adhesion wart
↔ Ripple crest line

1167

1168

1169   **Fig. 12.**

1170

1171

1172   **Fig. 13**

1173

1174   **Fig. 14**

1195 **Fig. 15**
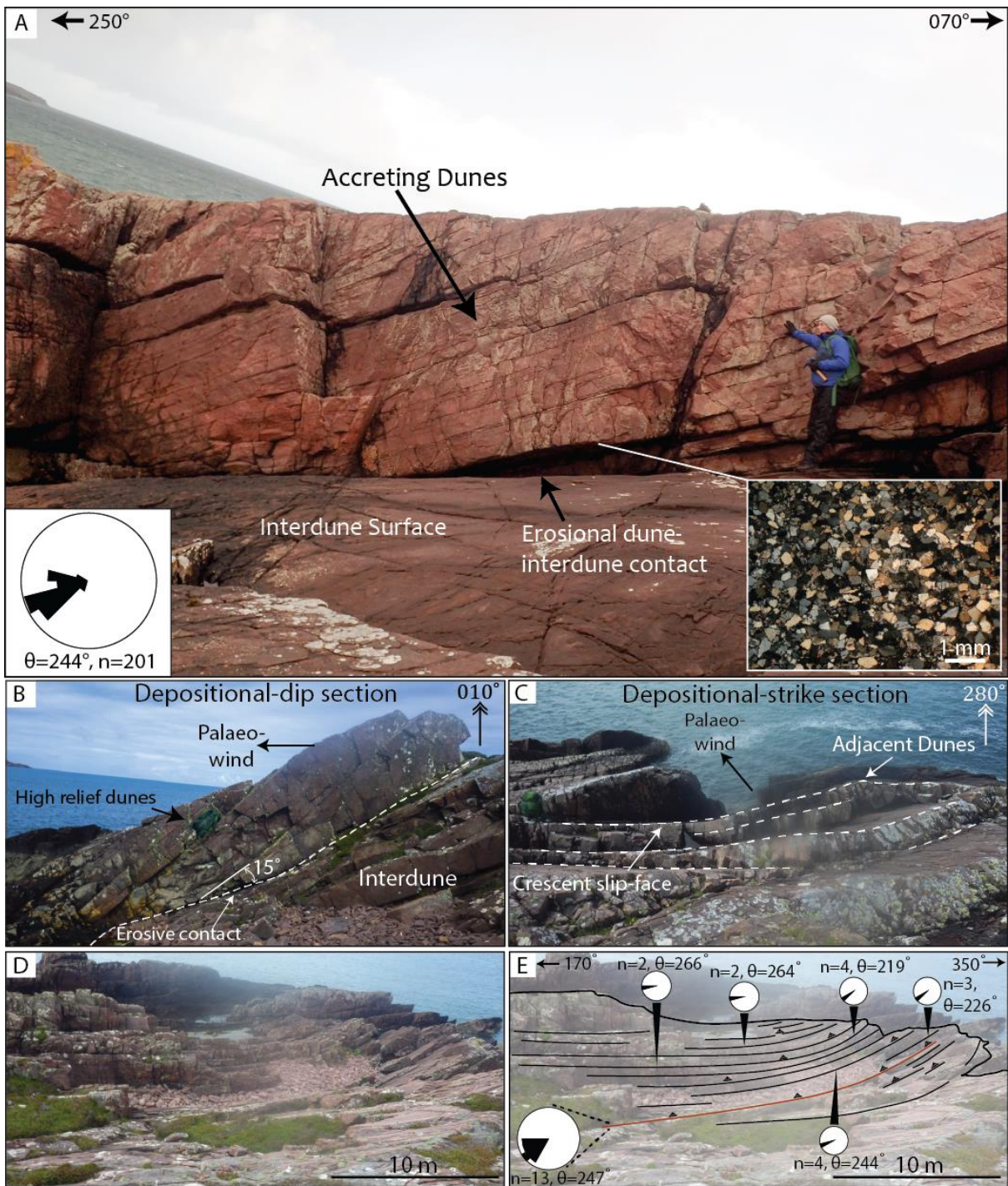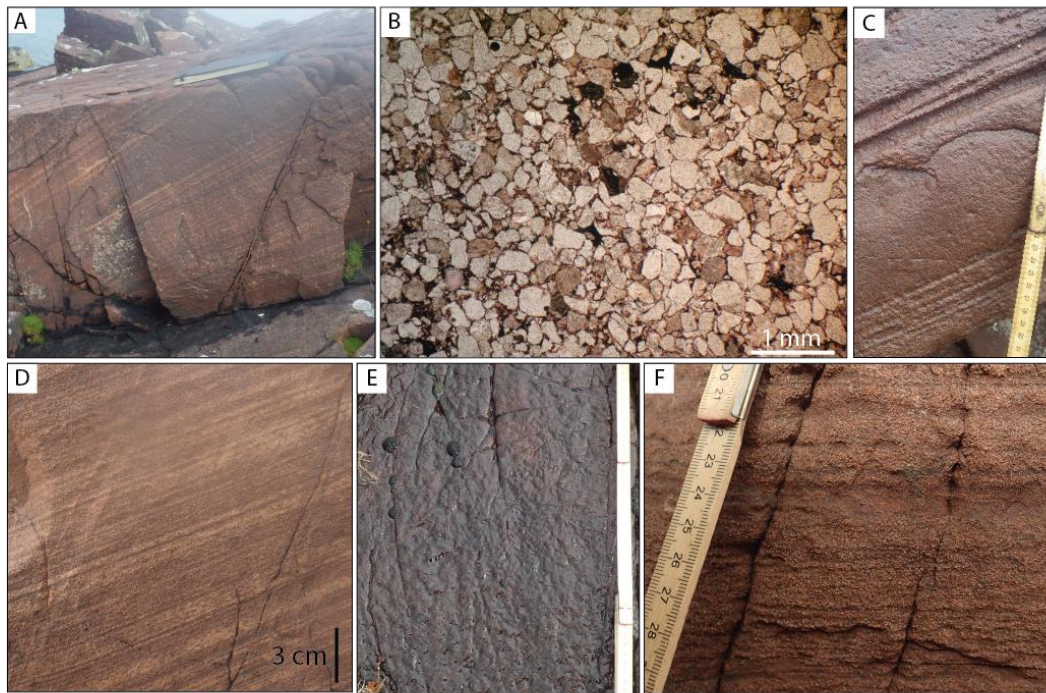
1201

1202 **Fig. 16.**

1203

1204 **Fig. 17**

1205

1206

1207

1208

1209

1210

1211

1212 **Fig. 18.**
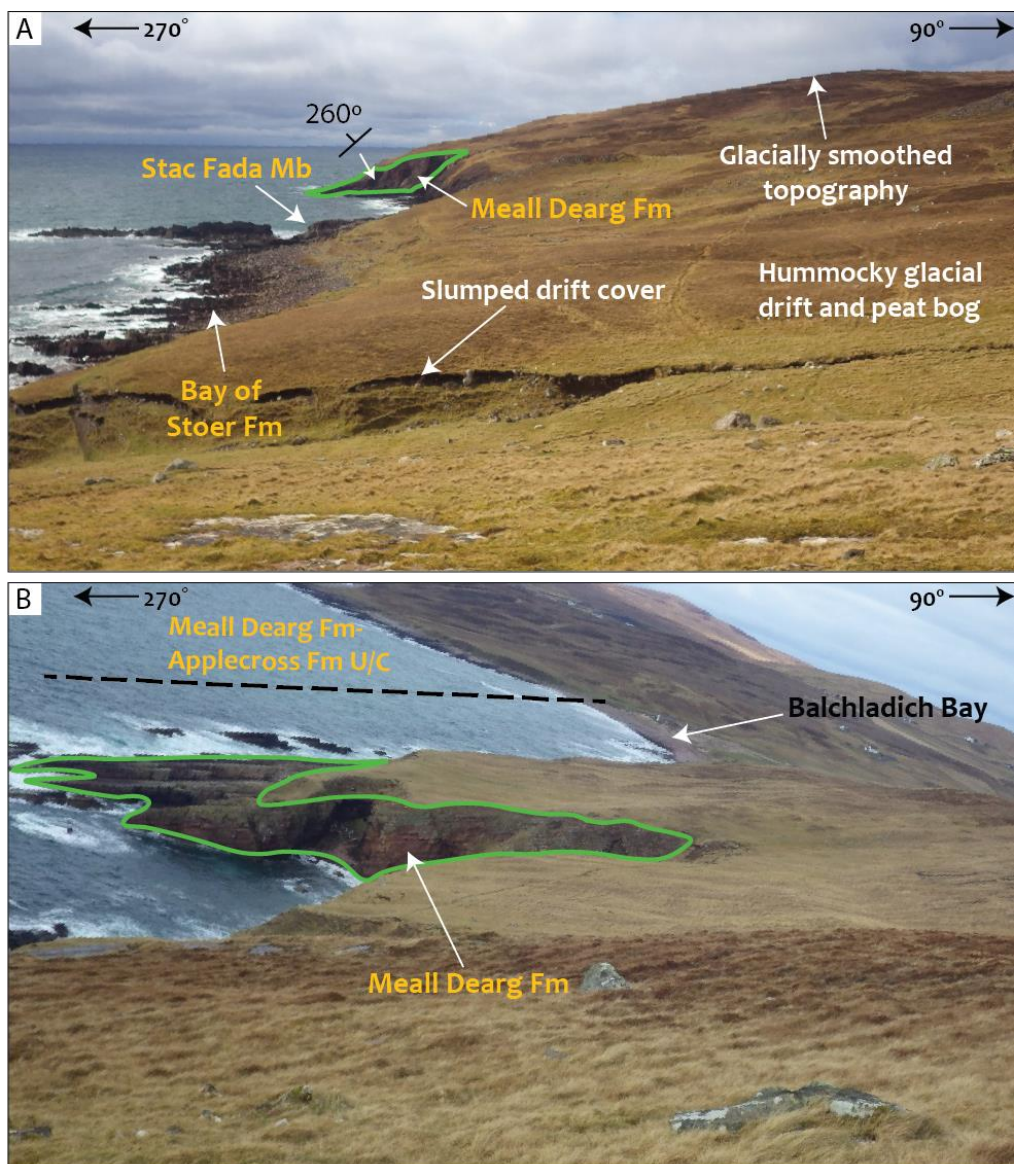

1213

1214

1215

1216

1217

1218

1219

1220

1221

1222

1223

1224   **Fig. 19.**

1225

1226

Table 1. Distribution of sedimentary structures across Meall Dearg locations. See text for information regarding frequency of occurrence.

Facies Association	Location	Type of exposure	Horizontal laminations	Antidune Stratification	Chute and Pool Structures	Humpback cross-stratification	Low angle cross-stratification	Planar cross-stratification	Trough cross-stratification	Ripple-marks	Adhesion marks	*Manchurio-phycus*	Reticulate marks	Planar Bedding
FA1	Stoer	Vertical cliffs	Y		Y		Y	Y	Y	Y	Y			
	Rubha Réidh	Stepped wave-cut platforms	Y	Y	Y	Y	Y	Y		Y	Y	Y	Y	
	Bachladich Bay	Stepped wave-cut platforms	Y	Y			Y	Y		Y	Y			
FA2	Enard Bay	Stepped wave-cut platforms						Y		Y				Y